NOTEBOOK PAPER

ISSN:1047-3289 *J. Air & Waste Manage. Assoc.* **59**:1258–1277
DOI:10.3155/1047-3289.59.11.1258

Deciphering the Role of Radical Precursors during the Second Texas Air Quality Study

Eduardo P. Olaguer
Houston Advanced Research Center, The Woodlands, TX; and the Texas Environmental Research Consortium, Houston, TX

Bernhard Rappenglück and Barry Lefer
Department of Atmospheric Chemistry, University of Houston, Houston, TX

Jochen Stutz
Department of Atmospheric and Oceanic Sciences, University of California–Los Angeles, Los Angeles, CA

Jack Dibb
Department of Tropospheric Chemistry, University of New Hampshire, Durham, NH

Robert Griffin
Department of Civil and Environmental Engineering, Rice University, Houston, TX

William H. Brune
Department of Meteorology, Pennsylvania State University, University Park, PA

Maxwell Shauck
Institute for Air Science, Baylor University, Waco, TX

Martin Buhr
Air Quality Design, Inc., Golden, CO

Harvey Jeffries and William Vizuete
Department of Atmospheric and Aquatic Sciences, University of North Carolina–Chapel Hill, Chapel Hill, NC

Joseph P. Pinto
U.S. Environmental Protection Agency, National Center for Environmental Assessment, Research Triangle Park, NC

ABSTRACT

The Texas Environmental Research Consortium (TERC) funded significant components of the Second Texas Air Quality Study (TexAQS II), including the TexAQS II Radical and Aerosol Measurement Project (TRAMP) and instrumented flights by a Piper Aztec aircraft. These experiments called attention to the role of short-lived radical sources such as formaldehyde (HCHO) and nitrous acid (HONO) in increasing ozone productivity. TRAMP instruments recorded daytime HCHO pulses as large as 32 parts per billion (ppb) originating from upwind industrial activities in the Houston Ship Channel, where in situ surface monitors detected HCHO peaks as large as 52 ppb. Moreover, Ship Channel petrochemical flares were observed to produce plumes of apparent primary HCHO. In one such combustion plume that was depleted of ozone by large emissions of oxides of nitrogen (NO_x), the Piper Aztec measured a ratio of HCHO to carbon monoxide (CO) 3 times that of mobile sources. HCHO from uncounted primary sources or ozonolysis of underestimated olefin emissions could significantly increase ozone productivity in Houston beyond previous expectations.

IMPLICATIONS

Texas was unable to demonstrate attainment of the 85-ppb ozone standard in Houston in its previous State Implementation Plan (SIP). The Houston SIP model was insufficiently productive in ozone despite an overabundance of NO_x and highly reactive volatile organic compound precursors. Enhancing the simulated efficacy of current control strategies by increasing radical sources in the SIP model base case and imposing future controls on radical precursors may enable Texas to demonstrate ozone attainment. Moreover, improving emissions and multiphase chemistry of radical precursors in SIP models will lead to better air quality management strategies.

Simulations with the CAMx model show that additional emissions of HCHO from industrial flares or mobile sources can increase peak ozone in Houston by up to 30 ppb. Other findings from TexAQS II include significant concentrations of HONO throughout the day, well in excess of current air quality model predictions, with large nocturnal vertical gradients indicating a surface or near-surface source of HONO, and large concentrations of nighttime radicals (~30 parts per trillion [ppt] HO_2). HONO may be formed heterogeneously on urban canopy or particulate matter surfaces and may be enhanced by organic aerosol of industrial or motor vehicular origin, such as through conversion of nitric acid (HNO_3). Additional HONO sources may increase daytime ozone by more than 10 ppb. Improving the representation of primary and secondary HCHO and HONO in air quality models could enhance the simulated effectiveness of control strategies.

INTRODUCTION

Texas Environmental Research Consortium and the Second Texas Air Quality Study

The Texas Environmental Research Consortium (TERC) is a nonprofit organization whose mission is to promote research that enables the state of Texas to demonstrate attainment of National Ambient Air Quality Standards, especially for 8-hr ozone (O_3). Two O_3 nonattainment areas of special interest to TERC are Dallas-Fort Worth (DFW) and Houston-Galveston-Brazoria (HGB). Since 2002, TERC has funded air quality research pertinent to these areas and the larger region of East Texas, addressing emission inventories, meteorology, atmospheric chemistry and transport, air quality modeling and monitoring, and control strategy evaluation. Olaguer et al.[1] have summarized the scientific and policy lessons learned from past TERC research.

TERC contributed significant funds to the Second Texas Air Quality Study (TexAQS II), a field campaign conducted mostly during the 2005 and 2006 O_3 seasons. TexAQS II was designed as a follow-up to the Texas Air Quality Study[2] of 2000 (TexAQS 2000 or TexAQS I), which was confined largely to Houston. Although TexAQS II devoted more resources to observations in other parts of East Texas than its predecessor study, the focus of this article is the preliminary scientific results and policy implications of TERC-funded projects in the Houston region during the 2006 intensive portion of TexAQS II. Cowling et al.[3] provide a related overview of TexAQS II, focusing on the activities of other agencies.

The TERC-funded portion of the TexAQS II intensive period in 2006 included real-time meteorological and air quality forecasts in support of daily flight planning for various airborne platforms (Nielsen-Gammon,[4] Byun et al.[5]), such as a heavily instrumented Orion P3 and an O_3 lidar-equipped Twin Otter operated by the National Oceanic and Atmospheric Administration (NOAA)[6]; mobile Solar Occultation Flux (SOF) measurements of volatile organic compounds (VOCs) in the Houston Ship Channel and other industrialized areas (Mellqvist et al.[7]); and the Houston Triangle Experiment (Berkowitz et al.[8]), in which measurements of O_3, particulate matter, and their precursors were conducted at three ground monitoring sites operated by the Texas Commission on Environmental Quality (TCEQ), namely Bayland Park, Deer Park, and Aldine. However, the main concern of this article is the TexAQS II Radical and Aerosol Measurement Project (TRAMP), conducted at the University of Houston Moody Tower,[9] and instrumented flights of the Baylor University Piper Aztec aircraft (Alvarez et al.[10]).

A special issue of the journal *Atmospheric Environment* is devoted to the scientific findings of the TRAMP study (e.g., Lefer et al.[11]). The purpose of this paper is not to duplicate that special issue but to concisely summarize in a single paper the main results of TERC-funded research during TexAQS II and their implications for the Texas State Implementation Plan (SIP) for the science and policy communities served by the Air & Waste Management Association.

Radicals and O_3 Productivity

The primary theme of this paper is the role of radicals in determining O_3 productivity in Houston. Radicals are molecular fragments that are highly reactive and unstable because of an unpaired valence electron. Hydroxyl (OH) is the most important atmospheric radical and is formed mostly by reactions between water vapor and excited oxygen atoms produced by O_3 photolysis. It can also be formed directly by photolysis of nitrous acid (HONO) and by reactions following the photolysis or oxidation of carbonyl compounds such as formaldehyde (HCHO) and other aldehydes. In addition, the reaction of excited states of nitrogen dioxide (NO_2) with water vapor was recently demonstrated by Li et al.[12] to be an important source of both hydroxyl radical and HONO.

Hydroxyl radicals react with VOCs to form HO_2 and other peroxy radicals, which convert nitric oxide (NO) emitted from sources to NO_2, regenerating OH in the process. NO_2 then photodissociates to form O_3 in the presence of molecular oxygen, while regenerating NO. These steps constitute a dual series of OH and NO chain reactions that produce O_3 from oxide of nitrogen (NO_x; including NO + NO_2).

The efficiency of O_3 production is determined by the abundance of radicals and NO_x and the chain lengths of the associated OH and NO regeneration cycles. These chain lengths are shortened by radical and NO_x termination reactions, including those that form radical reservoirs, such as hydrogen peroxide (H_2O_2), and NO_x reservoirs, such as nitric acid (HNO_3) and organic nitrates, which include peroxyacetyl nitrate (PAN) and peroxypropionyl nitrate (PPN). These long-lived reservoirs may later decompose and return radicals and NO_x to the atmosphere, often after being transported out of the airshed in which they were formed; they also may be lost entirely through deposition.

The 2006 8-hr O_3 SIP for the HGB nonattainment area was based on a historical O_3 episode in the summer of 2000. Jeffries et al.[13] have shown that the air quality model used for the 2006 HGB SIP underpredicts O_3 despite an overabundance of VOCs and NO_x compared with observations. The implied low O_3 productivity of the SIP model may be attributed to a dearth of new radicals, as opposed to internal radicals generated from decomposition of primary (emitted) and secondary (those produced

within the atmosphere) VOCs. Without additional sources of new radicals, most of the VOCs that are present in the model do not experience the initial decomposition that leads to O_3-producing chain reactions before leaving the Houston airshed through transport or deposition.

Vizuete et al.[14] analyzed an O_3 episode in the summer of 2006 and found that the radical limitation and associated inhibition of O_3 formation in the 2000 episode simulation may be significantly decreased by meteorological factors. These factors include an unusually high and rapidly growing planetary boundary layer (PBL), which reduces the termination of radicals by high surface concentrations of NO_x, and the entrainment of more aged air from above the PBL. The latter factor increases the efficacy of the larger radical pool by enabling less reactive VOCs to contribute more to O_3 production. Nevertheless, the anticipated impact of current O_3 control strategies in Houston is premised on the low O_3 production efficiency of the 2000 episode.

The relatively low O_3 productivity of the Houston SIP model was originally rather puzzling, because the model had large emission rates of highly reactive VOCs (HRVOCs), which are defined in the Texas SIP as the olefins ethylene, propylene, butenes, and 1,3-butadiene. HRVOCs are emitted in massive quantities from Houston Ship Channel petrochemical facilities during upsets and during scheduled maintenance, startup, or shutdown (Allen et al.[15]). These so-called "emission events" typically involve releases of HRVOCs from flares and cooling towers. HRVOCs may also be routinely emitted in large quantities from process vents and in fugitive releases. As a result of observations made during TexAQS I, HRVOCs are now thought to be responsible for rapid O_3 formation and hourly average concentrations approaching 200 parts per billion (ppb),[16] along with meteorological factors such as the stalling of sea breeze fronts.[17]

Although incorporation of additional base-case HRVOC emissions and an HRVOC cap-and-trade control strategy in the 2004 HGB SIP helped to demonstrate eventual attainment of the 1-hr O_3 standard by 2007, the most recent HGB SIP could not demonstrate attainment of the previous 85 ppb 8-hr O_3 standard by 2009, the deadline for moderate nonattainment areas. This prompted the governor of Texas to request a "double bump-up" for HGB to the severe nonattainment category, with an attainment deadline of 2018. The U.S. Environmental Protection Agency (EPA)'s recent downward revision of the 8-hr standard to 75 ppb makes the problem of O_3 attainment even more difficult for the Houston region.

Demonstration of O_3 attainment would be easier if the O_3 productivity of the underlying SIP model were increased, thus enhancing the simulated efficacy of current control strategies. This article presents some suggestive preliminary findings from TexAQS II that indicate where larger sources of radicals might be found and model results that gauge the potential impact of such sources on ambient concentrations of radicals and O_3 in Houston.

The findings described here are the result of initial data analysis efforts and model sensitivity studies. As such, they will inevitably be refined by further research, including a follow-up campaign to TexAQS II known as the Study of Houston Atmospheric Radical Precursors (SHARP). This TERC-funded field study was conducted mainly in April and May of 2009 and is focused primarily on the sources and atmospheric chemistry of radical precursors.

Prior Field Studies

Although TexAQS II laid considerably greater emphasis on the budget of radicals in Houston than TexAQS I, it was by no means the first field study to focus on this aspect of O_3 chemistry. For example, comprehensive measurements of radicals and the radical precursors HCHO and HONO were performed during the *Berlin Ozonexperiment* (BERLIOZ) campaign in July and August of 1998 (Platt et al.,[18] Alicke et al.[19]). During the 1999 Southern Oxidants Study (SOS) in Nashville, TN, HO_x radical (HO_2 + OH) concentrations and total OH reactivity were measured together with photolysis frequencies, NO_x, O_3, and many VOCs (Martinez et al.[20]). Measurements of HONO and other species using differential optical absorption spectroscopy (DOAS) were also performed during the SOS campaign (Stutz et al.[21]). In Taipei, DOAS measurements of HCHO were conducted in an air quality study between February and June 1999 (Matthew et al.[22]).

The original TexAQS I field study in 2000 consisted in part of measurements of the critical radical precursors HONO and HCHO. Heavily instrumented "supersites" were set up at La Porte Airport on the east side of Houston near the Ship Channel and Williams Tower on the non-industrial west side. A DOAS instrument was placed at La Porte and aimed at a retroreflector array on a water tower 1.9 km away to yield long-path average concentrations of HONO, NO_2, nitrate (NO_3), and O_3 (Stutz et al.[21,23]), as well as HCHO. In addition, a Nafion membrane diffusion scrubber (NMDS) instrument utilizing fluorometric Hantzsch cyclization chemistry was placed at the Houston Regional Monitoring site HRM-3 near the Ship Channel to measure HCHO (Dasgupta et al.[24]). Measurements of HCHO were also made aloft by tunable diode laser absorption spectroscopy (TDLAS) onboard the National Center for Atmospheric Research (NCAR) L-188C Electra aircraft (Wert et al.[25]).

Many other measurements were conducted during TexAQS I, notably of reactive alkenes such as ethylene and propylene (Ryerson et al.[16]), but for the sake of brevity are not discussed here. Relevant findings from this and other precursor field studies will be referred to in later sections of this article.

MEASUREMENT PLATFORMS

TRAMP

During TexAQS II, a supersite was set up on the south side of Houston (see Figure 1) as part of the TRAMP experiment. The goal of TRAMP was to answer the following questions:

(1) What are the main sources and sinks of radicals in the urban air of Houston?
(2) What processes determine the radical budget in the urban air of Houston?
(3) What secondary species are formed from reactions involving radicals?

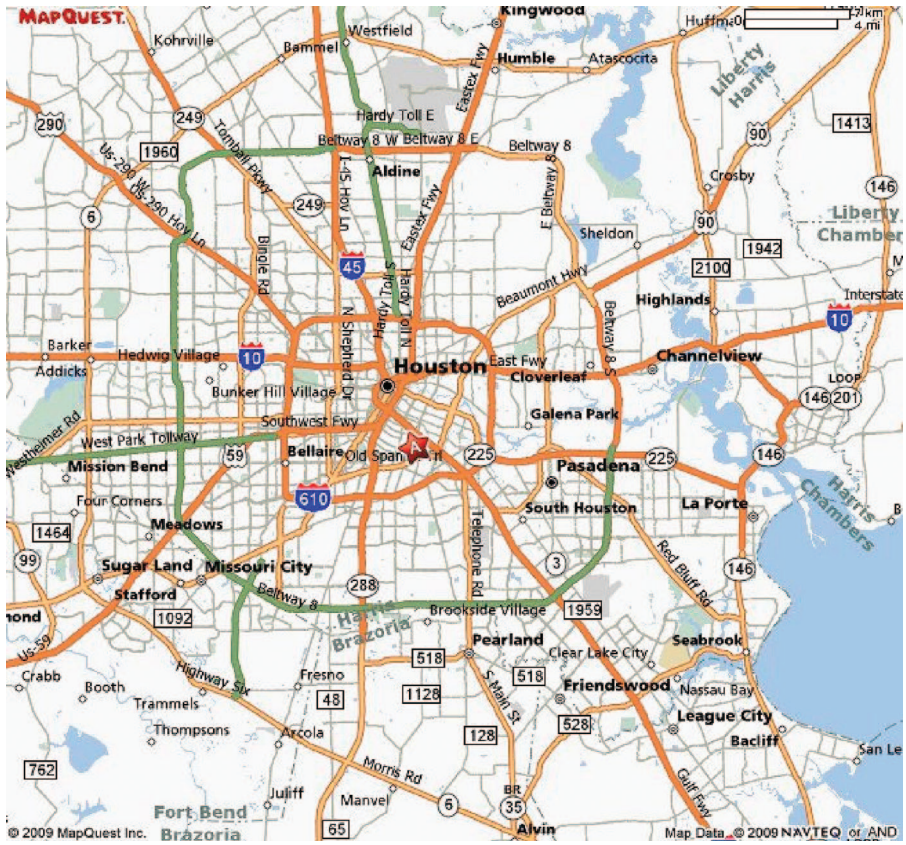

Figure 1. Location of Moody Tower (denoted by the red star) relative to the Houston Ship Channel, which is the body of water on the right-hand side of the diagram.

(4) What are the relative contributions of anthropogenic and biogenic emissions to O_3 and aerosol formation?

To address these issues, the University of Houston set up an air quality measurement facility on the roof of the 18-story tall North Moody Tower residence hall on its main campus. This facility included a 35-ft sampling tower and a wide variety of meteorological and chemical instruments. Table 1 provides a list of TRAMP measurement capabilities that resulted from collaborative arrangements with several academic and research institutions.

TRAMP measurements took place primarily during the months of August and September 2006, coinciding with most of the TexAQS II intensive period. Among the in situ monitoring techniques that yielded the most interesting preliminary results were Coil-Hantzsch reaction fluorescence (Coil-Hantzsch) measurements of HCHO, mist chamber ion chromatography (IC) observations of HONO and HNO_3, aerosol mass spectrometer (AMS) measurements of size-resolved aerosol composition, and laser-induced fluorescence (LIF) detection of HO_x radicals. In addition, the reactive nitrogen reservoirs PAN and PPN were measured using a gas chromatograph (GC) with an electron capture detector (ECD).

The commercial Coil-Hantzsch instrument obtained from Aerolaser measures HCHO by scrubbing it in a glass coil and detecting the fluorescent product of the reaction with ammonium acetate and acetyl acetone. Dasgupta et al.[24] summarized the results of intercomparisons between the Coil-Hantzsch method and other techniques for measuring HCHO, including DOAS and TDLAS. Similar measurement intercomparisons have been performed more recently by Apel et al.[26] and Wisthaler et al.[27]

The IC instrument, used to measure HONO and HNO_3, determines the concentrations of NO_3 and nitrite in the mist chamber solution. It is well established that HNO_3 overwhelmingly dominates the signal from NO_3 with no significant interference. On the other hand, soluble nitrite has been shown to include contributions from several NO_x species (e.g., pernitric acid [HNO_4] and perhaps organic nitrites/nitrates) in addition to HONO. Intercomparison of the IC and DOAS measurements of HONO made at Moody Tower yielded excellent agreement, except during occasional episodes when an unidentified interferant in the IC instrument led to discrepancies between the two techniques.[28]

An Aerodyne quadrupole AMS[29] was used to measure size-resolved mass concentrations of ammonium, NO_3, sulfate, chloride, and organic aerosol in submicron particles. The AMS data were corrected for instrumental collection efficiency using inorganic filter data (specifically, sulfate). Filter extracts were analyzed using IC.

LIF techniques were used to monitor HO_x radical concentrations. OH was measured by LIF, whereas HO_2 was determined by a ground-based tropospheric hydrogen oxides sensor (GTHOS), which measures HO_2 by LIF of OH following the chemical conversion of HO_2 to OH by adding NO.[30]

Table 1. List of measurements conducted during TRAMP.

Parameter	Measurement Instrument/Technique	Responsibility
Temperature	Campbell HMP45C	U. Houston [Lefer & Rappenglueck]
RH	Campbell HMP45C	U. Houston [Lefer & Rappenglueck]
Pressure	Campbell CS105	U. Houston [Lefer & Rappenglueck]
Rain amount/rate	Campbell TE525	U. Houston [Lefer & Rappenglueck]
Wind speed	Campbell 05103 R.M. Young	U. Houston [Lefer & Rappenglueck]
Wind direction	Campbell 05103 R.M. Young	U. Houston [Lefer & Rappenglueck]
O_3	UV photometry (TE 49C)	U. Houston [Lefer & Rappenglueck]
CO	Gas filter correlation (TE 48C TL)	U. Houston [Lefer & Rappenglueck]
NO, NO_2, NO_x	Chemiluminescence (TE 42C TL)/ BLD	U. Houston [Lefer & Rappenglueck]
C_2–C_{11} non-methane hydrocarbons	In situ GC-FID (Perkin Elmer)	U. Houston [B. Rappenglueck]
PAN, PPN, MPAN	In situ GC-ECD (Metcon)	U. Houston [B. Rappenglueck]
HCHO	Hantzsch reaction fluorescence	U. Houston [B. Rappenglueck]
H_2O_2	Liquid-phase reaction fluorescence	U. Houston [B. Rappenglueck]
Photolysis rates	SAFS	U. Houston [B. Lefer]
UV/VIS AODs, O_3 column	Brewer, CIMEL, UV-MFR, VIS-MFR	U. Houston [B. Lefer]
Cloud camera	Total Sky Imager (Yes, Inc.)	U. Houston [B. Lefer]
OH, HO_2, RO_2	GTHOS- LIF	Penn State University [B. Brune]
OH reactivity	MAOR—discharge flow tube LIF	Penn State University [B. Brune]
Turbulent heat flux	3-D Sonic anemometer	Penn State University [B. Brune]
NO, NO_x	Chemiluminescence (TE 42C)	Penn State University [B. Brune]
O_3	UV photometry (TE 49C)	Penn State University [B. Brune]
Oxy-VOCs	PTR-MS	Texas A&M [R. Zhang]
HNO_3, NO_3, N_2O_5	Ion drift-CIMS	Texas A&M [R. Zhang]
Aerosol size distribution	TDMA	Texas A&M [D. Collins]
Aerosol size distribution	SMPS, GRIMM, Streaker Impactor	Texas A&M [S. Brooks]
Aerosol backscatter remote sensing	Micropulse lidar	PNNL [C. Flynn]
SO_2	Pulsed fluorescence	NOAA—ARL [W. Luke]
NO_y	O_3 chemiluminescence	NOAA—ARL [W. Luke]
CO	Nondispersive Infrared	NOAA—ARL [W. Luke]
Elemental, particle bond and reactive gaseous Hg	Cold vapor atomic fluorescence (Tekran 2537a, 1130, 1135, and 1102)	NOAA—ARL [S. Brooks]
O_3, SO_2, NO_2, NO_3, HONO, HCHO	Long-path DOAS	UCLA [J. Stutz]
NO_2, HCHO	Vertical profiles via Max DOAS	UCLA [J. Stutz]
NO_2, HCHO	Vertical profiles via Max DOAS	Chalmers University [J. Mellquist]
CCN concentrations at different supersaturations, exposure times, and temperatures	Custom supersaturating column coupled to a phase-Doppler interferometer for drop sizing	University of California–Santa Cruz [P. Chuang]
Aerosol optical extinction and scattering coefficient, particle absorption coefficient, aerosol single-scattering albedo	Tandem CRDTN, TSI Model 3007 CPC	Portland State University [D. Atkinson]
Aerosol composition	AMS	UNH [R. Griffin]
Size-resolved mass concentration of organic carbon aerosol	Cascade impactors	UNH [R. Griffin]
Fine and coarse aerosol composition	Versatile air pollutant sampler (filter sampler)	UNH [R. Griffin]
Total number concentration of particles >7 nm in diameter	CPC	UNH [R. Griffin]
Water-soluble organic carbon gases and aerosols	Mist chamber collection and TOC analysis (Sievers 800 TOC Analyzer)	UNH [J. Dibb]
HNO_3, HONO	Mist chamber IC	UNH [J. Dibb]
$PM_{2.5}$ mass	TEOM	GaTech [R. Weber]
$PM_{2.5}$ organic and elemental carbon	Sunset Labs	GaTech [R. Weber]
$PM_{2.5}$ aerosol composition	PILS	GaTech [R. Weber]
$PM_{2.5}$ water-soluble organic carbon	PILS	GaTech [R. Weber]
HCHO, C_2H_4	Laser spectroscopy	Rice University [M. Fraser]
NO, O_3, aerosol scatter, total UV/VIS		Air Quality Design [M. Buhr]

Notes: AOD = aerosol optical depth, MPAN = peroxymethacryloyl nitrate, VIS = visible light, N_2O_5 = nitrogen pentoxide, CCN = carbyne, $PM_{2.5}$ = fine particulate matter, C_2H_4 = ethylene, TDMA = tandem differential mobility analyzer, SMPS = scanning mobility particle sizer, PILS = particle-into-liquid sampler, PNNL = Pacific Northwest National Laboratory, ARL = Air Resources Laboratory, U. Houston = University of Houston, UCLA = University of California–Los Angeles, UNH = University of New Hampshire, GaTech = Georgia Institute of Technology, SAFS = scanning actinic flux spectroradiometer, CRDTN = cavity ring-down transmissometer/nephelometer, CPC = condensation particle counter. Modified with permission from University of Houston.[9] Copyright 2007 TERC.

In addition to in situ monitoring, there were also long-path measurements using the DOAS technique. Using retroreflectors in conjunction with an active long-path DOAS (LP-DOAS) instrument, three light paths were set up to measure horizontal average concentrations between Moody Tower and downtown Houston. Observations were averaged in the vertical in the following height intervals: 20–70 m (lower), 70–130 m (middle), and 70–300 m (upper). With this technique, vertical gradients of O_3, NO_2, NO_3, sulfur dioxide (SO_2), HCHO, and

Table 2. Baylor Aztec instrumentation package.

Parameter (units of measure)	Method Name or Published Reference	Analytical Technique	Sample Period (sec)	Detection Limit (units ppb unless otherwise stated)
O_3 (ppbv)	NA	Dual-beam UV absorption	1-sec poll of 2-sec updates	2
NO (ppbv)	40 CFR 58	Chemiluminescence	1-sec poll of 2-sec updates	2
NO_2 (ppbv)	40 CFR 58	UV photolysis with chemiluminescence	1-sec poll of 2-sec updates	2
NO_y (ppbv)	NA	Molybdenum catalytic sample reduction at 320 °C and chemiluminescence	1-sec poll of 2-sec updates	2
SO_2 (ppbv)	40 CFR 58	Pulsed fluorescence	1-sec poll of 2-sec updates	2
CO (ppbv)	NA	Vacuum UV fluorescence	1-sec poll of 2-sec updates	2(τ = 10 sec)
Reactive alkenes (alkenes in ppbv)	NA	Chemiluminescence	1	1
VOCs (C_2–C_9)	NA	GC and FID	Whole air samples (~1 min)	10 pptv
HCHO	NA	Hantzsch reaction	1-sec poll of 1-sec updates	50 pptv
Particle light scattering (sp and bsp $\times$ $10^- \cdot m^{-1}$) red, green, and blue wavelengths	NA	3λ nephelometry (TSI)	1	$1 \times 10e^{-6} \cdot m^{-1}$
Particle counter (testing only; counts/L) 0.2–30 μm	NA	Light scattering	1-sec poll of 6-sec updates	1 particle/L
j(NO_2)[photolysis frequency of NO_2]	NA	Upward- and downward-pointing filter radiometers (actinic flux)	1	NA
Altitude (ft above mean sea level)	NA	GPS	1	1 ft
Latitude and longitude (degrees, min, sec)	NA	GPS	1	0.04 sec of latitude and/or longitude
Wind direction (degrees azimuth)	NA	Inferred from aircraft motion	1	5°
Wind speed (knots/m $\cdot$ sec^{-1})	NA	Inferred from aircraft motion	1	5 Knots (2.55 m/sec)
Temperature (°C)	NA	Aspirated platinum resistance	1	0.01 °C
RH (%, absolute)	NA	Solid state sensor	1	0.1%

Notes: ppbv = parts per billion by volume, pptv = parts per trillion by volume, CFR = *Code of Federal Regulations*, GPS = Global Positioning System. Modified with permission from Alvarez et al.[10] Copyright 2007 TERC.

HONO were obtained in the lowest 300 m of the atmosphere. A second instrument, known as a multiaxis differential optical absorption spectrometer (MAX-DOAS), used passive absorption of scattered solar radiation along eight elevation-viewing angles during daytime to measure vertical profiles of NO_2 and HCHO. The viewing direction was approximately parallel to that of the LP-DOAS.

The Baylor Aztec Flights

An instrumented Piper Aztec aircraft was deployed by Baylor University in support of several experiments during TexAQS II, including the TRAMP and SOF experiments. In addition to collecting whole air samples using canisters for later measurement of VOC concentrations using GC with flame ionization detection (FID), the Aztec's in situ instrumentation package included several fast measurement devices. These are listed in Table 2.

Of special interest is the Coil-Hantzsch instrument deployed on the Aztec, which is identical to the one deployed at Moody Tower. This instrument was calibrated with an aliquot liquid standard from Aerolaser at the beginning of the field study and intercalibrated with the Moody Tower instrument using a gas standard from the NCAR at the end of the study. During the field study the instrument was challenged with gaseous HCHO from its internal permeation tube to demonstrate stability and track step changes.

Also onboard the Aztec was a reactive alkene detector (RAD) that measured total unspeciated HRVOCs (plus other olefins). This is a chemiluminescence instrument calibrated for response to ethylene, propylene, butadiene, and isoprene, with results reported as equivalents of propylene. Multipoint calibrations of the RAD were conducted with propene, a National Institute for Standards and Technology (NIST) traceable gas standard from Scott Marrin, Inc. before each flight and off-day calibrations.

The Aztec flew a total of 50 hr for TERC, mostly in the Houston region but also in the vicinity of a stationary front near the DFW area during an O_3 exceedance. In addition, the aircraft was deployed outside Houston and Dallas to investigate long-range transport of pollution. This latter experiment was funded by the Northeast Texas Air Care group of stakeholders.

DATA OVERVIEW

Two Interesting Days

The chemical and meteorological conditions during the 2006 TRAMP experiment, including several high O_3 episodes, were surveyed by Lefer et al.[11] The TRAMP time period was more representative of the climatology from 2000 to 2007 than the unusually hot conditions prevailing during TexAQS I in 2000. Although the TexAQS II intensive period in 2006 coincided with several intriguing O_3 episodes, it is the intention of the authors

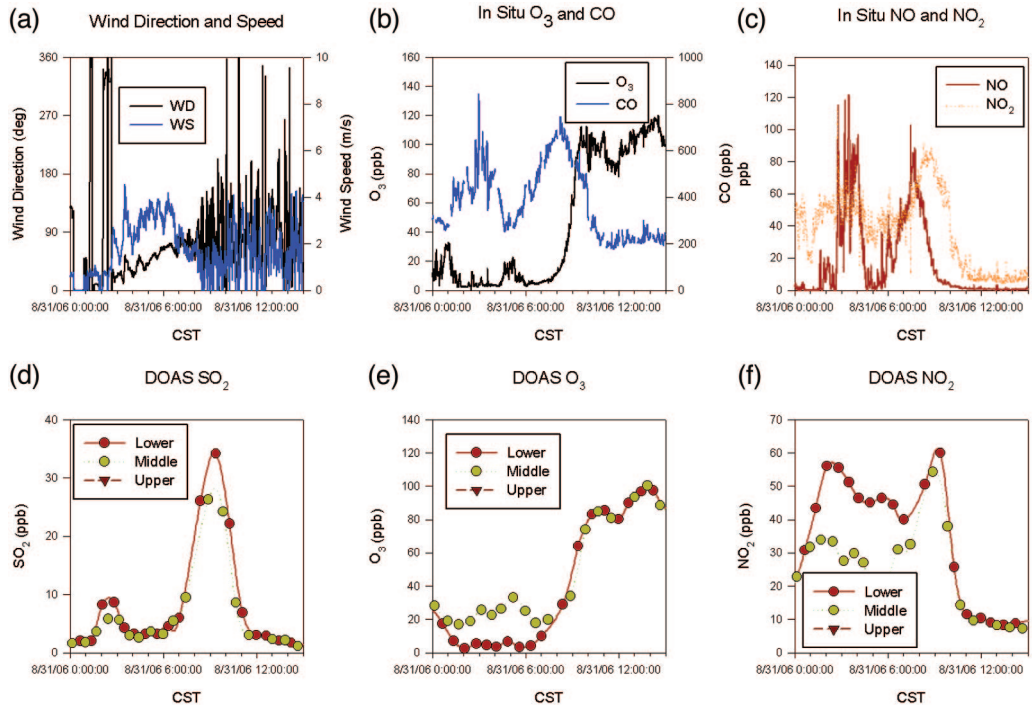

Figure 2. Measurements of (a) local wind speed and direction, (b) in situ O_3 and CO, (c) in situ NO and NO_2, (d) DOAS SO_2, (e) DOAS O_3, and (f) DOAS NO_2 from 12:00 a.m. through the afternoon of August 31, 2006 on Moody Tower. Note that data for the upper path of the DOAS were missing on this day.

not to give a comprehensive description of the attendant phenomena but to call attention to a few key issues highlighted by certain observations. In this respect, there were two very interesting days that deserve emphasis, namely August 31, 2006 and September 14, 2006. The relevant observational data collected at Moody Tower and by the Baylor Aztec are discussed in the following subsections.

August 31, 2006. Figures 2 and 3 display data collected at Moody Tower from 12:00 a.m. to 3:00 p.m. on August 31, 2006. These data include (1) local wind direction and

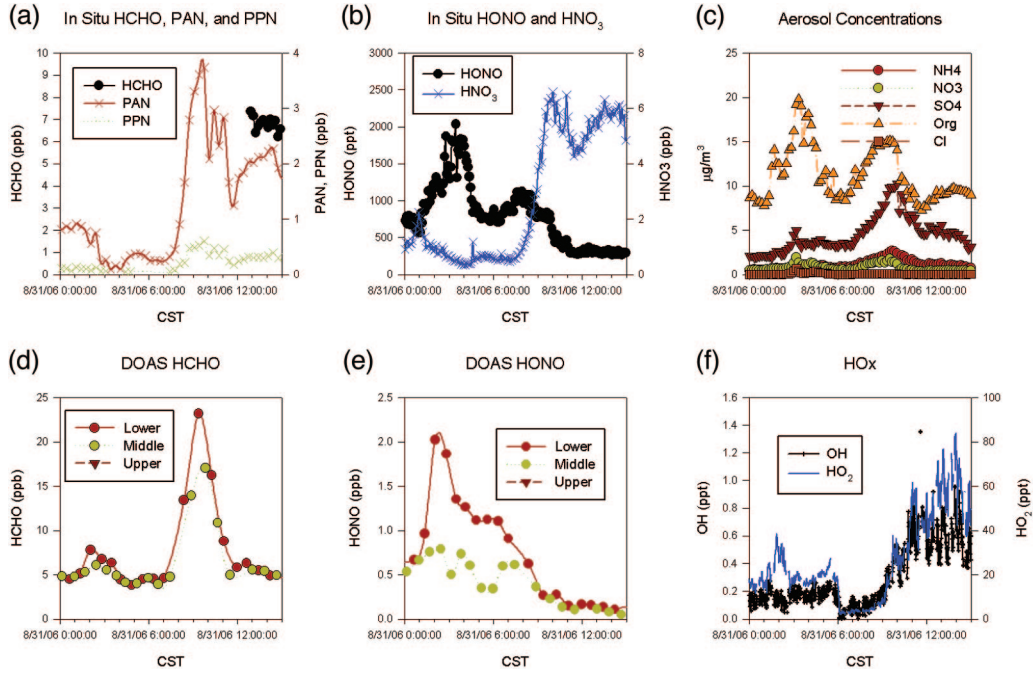

Figure 3. Measurements of (a) in situ HCHO, PAN, and PPN; (b) in situ HONO and HNO_3; (c) aerosol concentrations; (d) DOAS HCHO; (e) DOAS HONO; and (f) HO_x radical concentrations from 12:00 a.m. through the afternoon of August 31, 2006 on Moody Tower. Note that data for the upper path of the DOAS were missing on this day.

speed; (2) in situ O_3 and CO; (3) in situ NO and NO_2; (4) DOAS SO_2; (5) DOAS O_3; (6) DOAS NO_2; (7) in situ HCHO, PAN, and PPN; (8) in situ HONO and HNO_3; (9) aerosol concentrations; (j) DOAS HCHO; (k) DOAS HONO; and (l) HO_x radical concentrations.

On the night of August 31, the DOAS lower path recorded a burst of HONO (2 ppb) around 2:00 a.m. when the local wind was stagnant. There was clearly a gradient of HONO with smaller values (<1 ppb) aloft throughout the early morning, indicating a surface source of HONO. The DOAS HONO spike at 2:00 a.m. was accompanied by spikes in HO_2 (40 parts per trillion [ppt]) and DOAS NO_2 (56 ppb). The IC instrument recorded an in situ HONO spike of 2 ppb at 3:30 a.m., which appears to be closely linked with a spike in AMS-measured organic aerosol and in situ NO_x and CO at about the same time. DOAS lower path and in situ O_3 were depressed below 10 ppb from 12:00 a.m. to early morning, as the result of NO emissions and the reaction $NO + O_3 \rightarrow NO_2 + O_2$, as well as surface deposition and weak vertical mixing in the nighttime boundary layer. The combination of these factors resulted in a strong positive gradient of O_3 (up to 40 ppb) at night.

On the morning of August 31, an O_3 exceedance was observed to occur on the west side of Houston, probably as a result of petrochemical industry emissions from the Houston Ship Channel on the east side of the city. The wind direction data of Figure 2 show a prevailing northeasterly wind. This wind likely transported Ship Channel emissions of HRVOCs and their secondary byproducts, including HCHO and O_3, toward the southwest. At that time, the Baylor Aztec aircraft, whose flight paths during TexAQS II are shown in Figure 4a, observed stratified layers over downtown Houston and to the west of Houston, with peak O_3 mixing ratios of approximately 177 ppb near the downwind transects of the Ship Channel.

The Aztec flight trajectory on August 31 is depicted in Figure 4b, which also shows the variation of HCHO observed along the flight path. Unfortunately, the Coil-Hantzsch instrument was unable to measure HCHO above 15 ppb because of data cutoff issues. However, concentrations beyond this threshold were indicated by the Aztec measurements in the vicinity of the Ship Channel, where there are large emissions of O_3 precursors. An example of this is presented in Figure 5, which shows plumes of HRVOC (denoted by RAD, referring to the propylene equivalent concentration of the measured reactive alkenes), total reactive nitrogen (NO_y; NO_x + nitrogen reservoirs), CO, and SO_2 coincident with the plumes of HCHO, especially between 8:15 a.m. and 8:30 a.m.

The observations from Moody Tower during the late morning of August 31 shown in Figures 2 and 3 are consistent with the Baylor Aztec observations. Around 9:20 a.m. of August 31, the DOAS lower path recorded a burst of HCHO (23 ppb), whereas the DOAS middle path also recorded high HCHO (>15 ppb) at the same time. The HCHO peak at 9:20 a.m. was accompanied by a spike in DOAS SO_2 (34 ppb lower path, 24 ppb middle path) and in PAN (3.6 ppb). In situ NO and CO likewise peaked around that time. The SO_2 spike indicates that the HCHO peak may be the primary or secondary result of industrial emissions from the Ship Channel. For example, HCHO

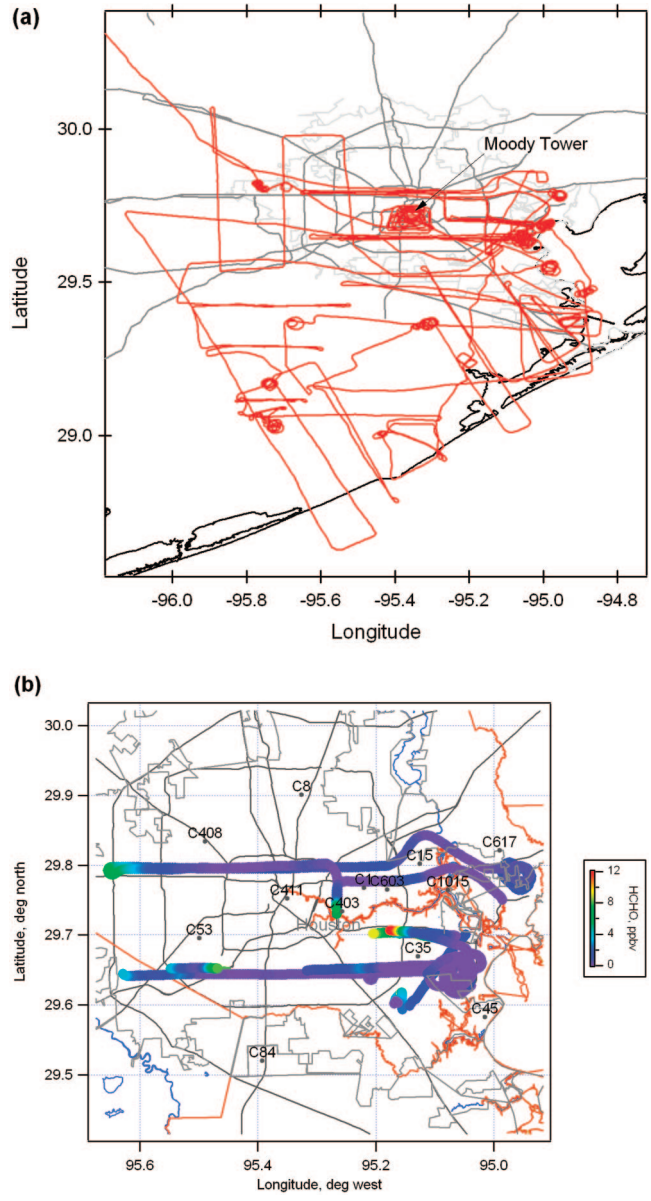

Figure 4. (a) Flight paths of Baylor Aztec in Houston during TexAQS II in 2006. (b) Flight path for Baylor Aztec aircraft on the morning of August 31, 2006 and concentrations of HCHO measured by the Coil-Hantzsch method. Modified with permission from Alvarez et al.[10] Copyright 2007 TERC.

emissions from natural gas flares may occur at roughly the same time, although not necessarily at the same immediate location, as refinery emissions of SO_2 from sulfur processing, power generation, and process gas flares. Likewise, the observed large values of PAN may be a byproduct of industrial HRVOC and NO_x from the Ship Channel. O_3 rose above 60 ppb at the time of the HCHO peak at 9:20 a.m. and eventually reached 140 ppb at the Moody Tower site in the late afternoon. The O_3 increase at this time may have been aided by a shift in wind direction from northeasterly to southeasterly and the associated trapping or recirculation of polluted air.

September 14, 2006. Figures 6 and 7 display similar plots of observations collected at Moody Tower as in Figures 2 and 3,

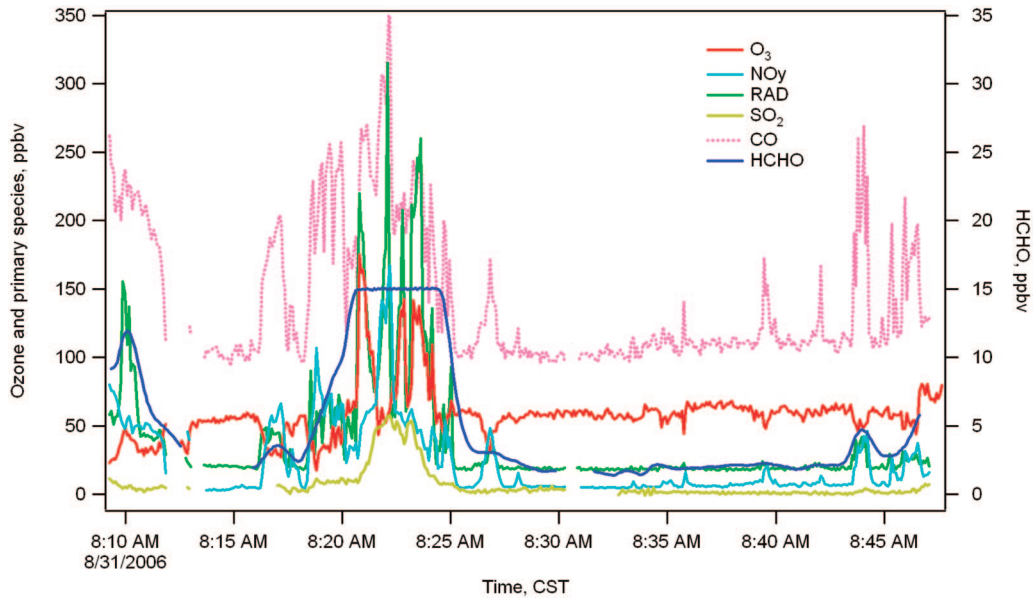

Figure 5. Baylor Aztec measurements of O_3 and several primary species on the morning of August 31, 2006. RAD denotes the propylene equivalent concentration (in ppb) measured by the RAD. Modified with permission from Alvarez et al.[10] Copyright 2007 TERC.

except that they are for September 14, 2006. The local wind at Moody Tower was largely northeasterly or easterly on September 14. Transport of an SO_2 plume aloft appeared to occur beginning a few hours after 12:00 a.m. The DOAS SO_2 data suggest that vertical mixing may have brought the elevated plume down to the surface by late morning. HONO remained elevated at approximately 1 ppb through the night and early morning. HONO then decreased slowly to several hundred ppt during the afternoon. Once again, a surface source of HONO is indicated by the negative vertical gradient in the DOAS observations.

O_3 was extremely low during the morning rush hour, coincident with the peaks in CO and NO, indicating strong titration by mobile sources. Despite this, in situ

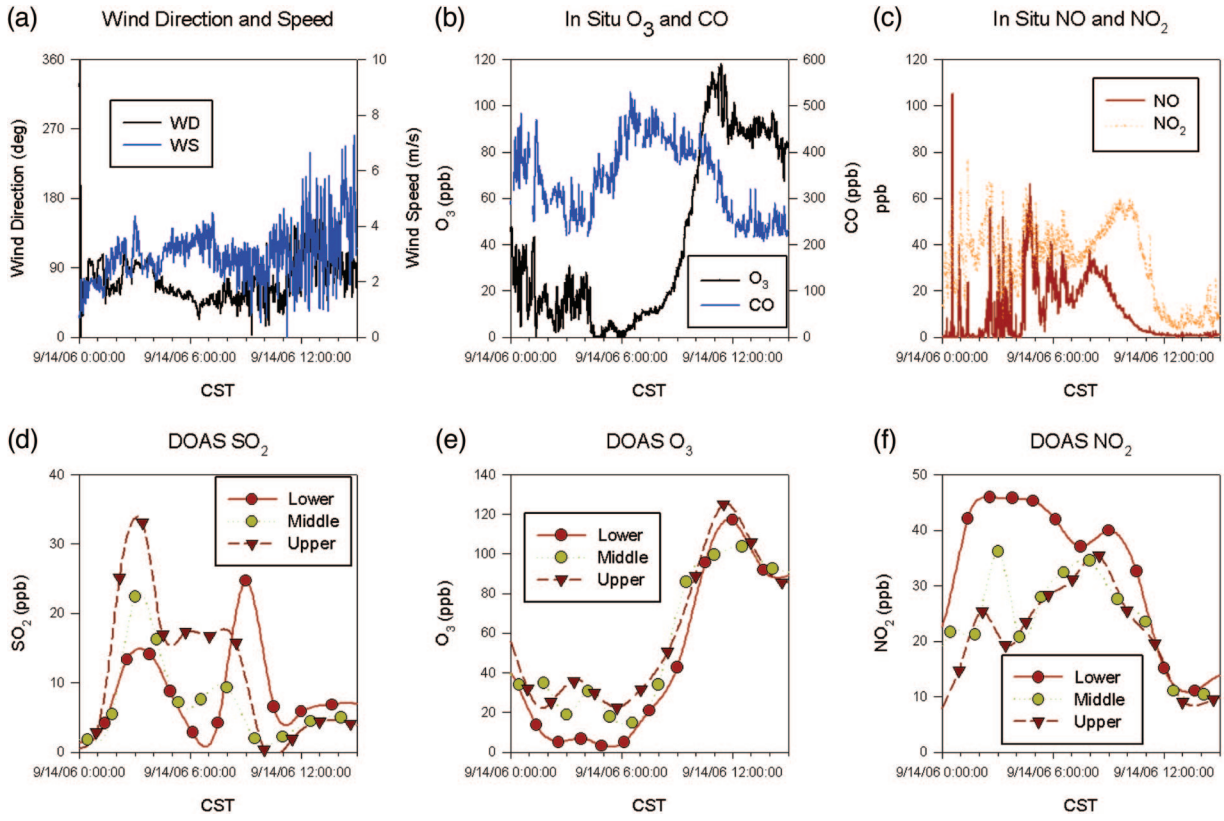

Figure 6. Measurements of (a) local wind speed and direction, (b) in situ O_3 and CO, (c) in situ NO and NO_2, (d) DOAS SO_2, (e) DOAS O_3, and (f) DOAS NO_2 from 12:00 a.m. through the afternoon of September 14, 2006 on Moody Tower.

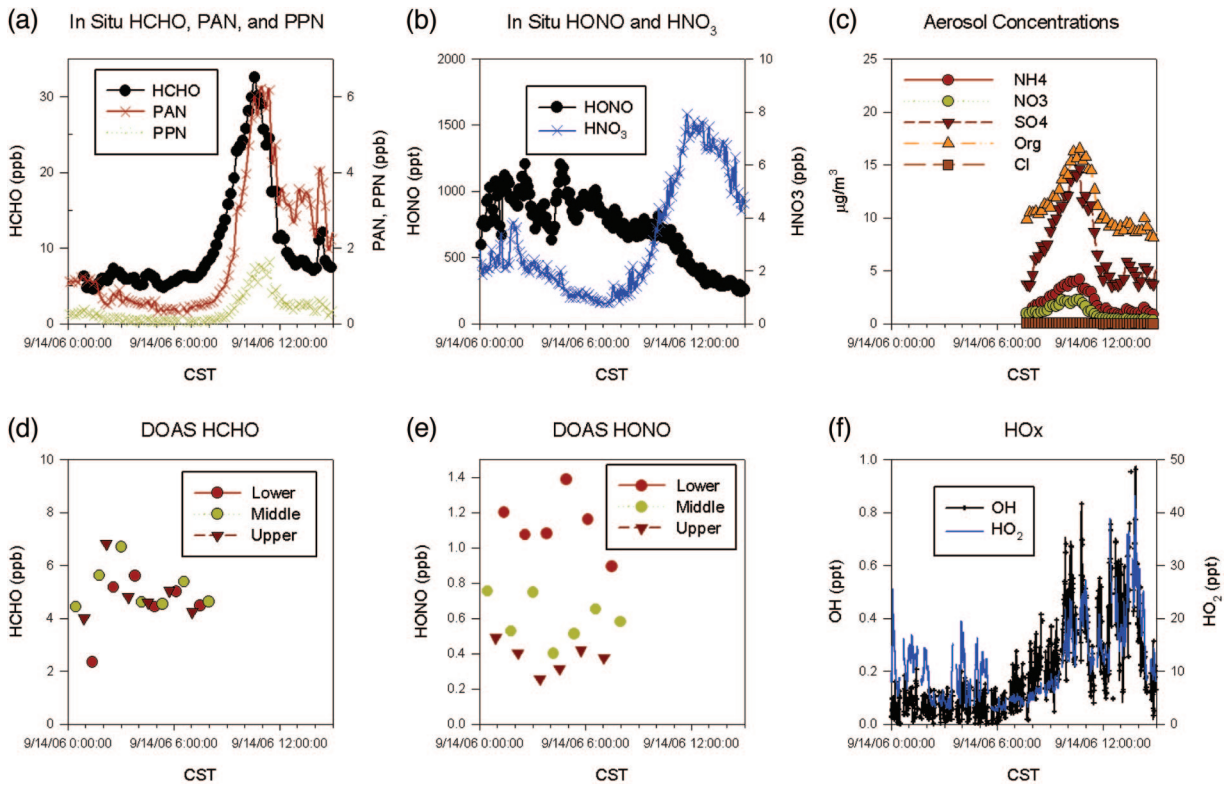

Figure 7. Measurements of (a) in situ HCHO, PAN, and PPN; (b) in situ HONO and HNO_3; (c) aerosol concentrations; (d) DOAS HCHO; (e) DOAS HONO; and (f) HO_x radical concentrations from 12:00 a.m. through the afternoon of September 14, 2006 on Moody Tower.

and DOAS O_3 peaked at approximately 120 ppb around 12:00 p.m. The O_3 peak was accompanied by bursts in HO_x and HNO_3 (8 ppb), as expected from typical daytime photochemistry. This was preceded by a late morning burst of HCHO (32 ppb) and PAN (6 ppb), organic and sulfate aerosol (15 $\mu g/m^3$), and HO_x. Before that, there were mid-morning increases in NO_2 and SO_2, accompanied by yet another HO_x pulse. In situ HONO at mid-morning was persistently above 700 ppt.

HCHO

Primary versus Secondary HCHO. During TexAQS I, the ground-based NMDS instrument located near the Ship Channel detected HCHO concentrations that ranged from a minimum of 150 ppt to a maximum of 47 ppb, with mean and median concentrations of 4.5 and 3.3 ppb, respectively (Dasgupta et al.[24]). Airborne TDLAS measurements of HCHO likewise exceeded 30 ppb on some occasions, with concentrations of HCHO routinely 10–20 ppb above background whenever O_3 exceeded 120 ppb (Wert et al.[25]).

During TexAQS II, multiple instruments at Moody Tower and on the Baylor Aztec clearly saw unusually large HCHO concentrations on par with those observed during TexAQS I, such as in the late morning of September 14, 2006 when HCHO reached 32 ppb. Although that HCHO peak was the largest observed at Moody Tower during the TRAMP study, it was not the largest HCHO concentration observed during the entire TexAQS II campaign. A Hantzsch-based instrument operating at Lynchburg Ferry in the Houston Ship Channel recorded a HCHO peak of 52 ppb at approximately 9:20 a.m. of September 27, 2006 (Eom et al.[31]). The largest nighttime HCHO peak recorded at Moody Tower was 14 ppb and was observed at approximately 12:00 a.m. of September 19–20, 2006.

There are four hypotheses that can possibly explain the large plumes of HCHO seen during both TexAQS campaigns: (1) direct emissions, (2) daytime OH-driven secondary formation within Houston, (3) nocturnal or daytime formation from ozonolysis of industrial olefins from the Ship Channel, and (4) transport of biogenically formed HCHO from isoprene degradation outside of Houston. Of these hypotheses, only the first involves primary HCHO. A vital question for control strategies is the extent to which HCHO peaks in Houston are primary or secondary in origin.

Before TexAQS II, Friedfeld et al.[32] examined statistical correlations between HCHO and CO (an indicator of primary HCHO) and between HCHO and O_3 (an indicator of secondary HCHO). Their work suggested that approximately 37% of total HCHO in Houston could be primary. A similar average value (39%) was obtained from multiple regression analyses of TRAMP data by Rappenglück et al.,[33] who found a pronounced diurnal variation in primary HCHO. During morning rush hour, the contribution of CO-associated HCHO reached almost 75% and then dropped below 10% during the daytime when secondary HCHO was dominant. In addition, Rappenglück et al.[33] found that, on average, 9% of Houston HCHO was associated with SO_2. This SO_2-associated HCHO occurred almost exclusively after the breakup of the morning inversion layer, and its contribution to total HCHO at times peaked at approximately 67%. This pronounced correlation

Table 3. Measured emission rates obtained by SOF and the 2004 Texas emissions inventory for non-methane hydrocarbons.[a]

Species	Ethene (kg/hr)		Propene (kg/hr)		Alkanes (kg/hr)		Total VOCs (kg/hr)
Area	Measured	Inventory	Measured	Inventory	Measured	Inventory	Inventory
Ship Channel	860	47	1,500	61	12,400	1,500	3,090
Mt. Belvieu	404	44	400	9	860	260	265
Baytown	72	6	260	3	980	202	437
Texas City	83	8	–	–	2,890	348	686
Channelview	64	11	–	–	–	42	170
Sweeny	163	4	126	4	3,630	113	137
Freeport	250	21	–	–	–	44	148
Bayport	170[b]	4	–	–	–	94	151
Chocolate Bayou	136[b]	10	273	24	–	107	150

Notes: [a]Nonmethane hydrocarbons corresponding to alkanes and unspeciated VOC as in the 2004 inventory; [b]Uncertain because of few measurements. Modified with permission from Mellqvist et al.[7] Copyright 2007 TERC.

might indicate an industrial primary or secondary source of HCHO.

Wert et al.[25] examined TDLAS data from the NCAR Electra that flew during TexAQS I and were able to distinguish plumes originating from the Ship Channel from those coming from power plants or mobile sources. The Ship Channel plumes were discriminated from others by their greatly enhanced HCHO and O_3 production and stronger correlations and ratios between HCHO and the tracers O_3 and NO_y. Using a reactive Lagrangian plume model with specified emissions of biogenic isoprene and only two anthropogenic non-methane hydrocarbons—namely ethylene and propylene (at levels far larger than reported in emissions inventories)—Wert et al.[25] were able to reproduce airborne observations of HCHO without recourse to direct emissions of HCHO for isolated petrochemical facility plumes and amalgamated Ship Channel plumes. Moreover, Wert et al.[25] did not detect levels of HCHO significantly above background near isolated facilities with routine emissions, suggesting the absence of significant primary HCHO. However, their conclusions are limited by the relative simplicity of the Lagrangian plume model, variable meteorology, limited VOC sampling, and the possibility of primary HCHO from nonroutine industrial emissions.

Dasgupta et al.[24] reported TexAQS I measurements of HCHO from the ground-based NMDS instrument at HRM-3 that were much in accord with those of Wert et al.[25] On all days when HCHO exceeded 25 ppb, back trajectories indicated an origin within the Ship Channel. Strong daytime peaks were correlated with O_3 and HNO_3 (suggesting OH-driven chemistry) and often with SO_2 as was also observed during TexAQS II. However, there was an unusual 15-ppb HCHO peak around 12:00 a.m. of September 17–18, 2000 that suggested a large source of primary HCHO. O_3 at this time was titrated to zero by very large NO emissions that occurred simultaneously with the HCHO peak.

There is the possibility that, on some nights as well as during the day, unusual amounts of HCHO may be secondarily produced from reactions between O_3 and industrial olefins emitted in the Ship Channel, if the O_3 is not titrated away by co-emitted NO. This might occur during noncombustion releases, such as olefin emissions from fugitives, cooling towers, or deheading cokers. Emission fluxes measured by the mobile SOF instrument in the Ship Channel during TexAQS II indicate that olefins and other VOCs may be underestimated in the Houston emissions inventory by an order of magnitude or more (see Table 3).[7]

During the day, one would expect considerable OH-driven secondary production of HCHO to result from large emissions of olefins and other VOCs. The simultaneous peaks in PAN and PPN often accompanying daytime HCHO peaks in the TRAMP data (as exemplified by August 31, 2006 and September 14, 2006) are certainly an indication that secondary formation of HCHO is active, because PAN and PPN are co-products of VOC decomposition leading to the formation of aldehydes. However, analysis of the Baylor aircraft data for the morning of August 31, 2006 by Alvarez et al.[10] indicates that there may be a significant primary component of daytime peak HCHO. Figure 8 shows that large concentrations of

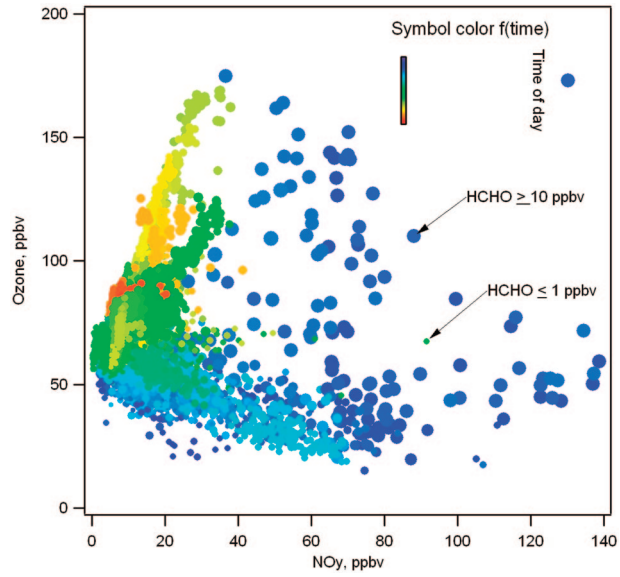

Figure 8. Baylor Aztec data showing relationships between O_3, NO_y, and HCHO. The symbol color indicates flight time (blue denoting earlier time, red denoting later time), whereas the symbol size indicates the amount of measured HCHO. Modified with permission from Alvarez et al.[10] Copyright 2007 TERC.

HCHO observed by the Aztec often coincided with small O_3 and large NO_y mixing ratios. These larger HCHO concentrations typically occur closer to Houston Ship Channel sources (see Figure 4). The warmer colors in Figure 8 indicate photochemically aged air with high O_3 and relatively low HCHO.

Much analysis remains to be done to determine the relative importance of primary and secondary HCHO on the basis of measurements performed during TexAQS II. This includes analysis of data collected not only by TERC-funded investigators, but also onboard the Orion P3 aircraft and the Research Vessel *Ronald H. Brown*.[3,6]

Possible Missing Sources of HCHO. What sources might contribute significantly to primary HCHO beyond those already taken into account in current emissions inventories? A major suspect is flaring from petrochemical facilities in the Ship Channel, as was hypothesized by Dasgupta et al.[24] to explain the large midnight spike in HCHO on September 18, 2000. It is possible that incomplete combustion of VOCs in flares could produce significant amounts of HCHO, a hypothesis that has yet to be seriously tested in computational models of flare emissions or, before the SHARP campaign in 2009, by direct observations in the field. However, measurements of HCHO produced from refinery fuel gas in a research burner at Sandia National Laboratory were conducted as part of the Petroleum Research Forum's Project 92-19 (Seebold et al.[34]). In that project, superstoichiometric conditions resulted in flue gas concentrations of HCHO of approximately 1 ppm, similar to the concentrations of co-produced ethylene and propylene.

Current emission model representations of flares do not even distinguish among different facility types, such as olefin plants and refineries. A uniform destruction efficiency of 99% is usually applied to a standard input stream, without accounting for the chemical processing within the flare. In a combustion modeling study, Castineira and Edgar[35] found that high-momentum flames, which can occur during upset conditions of industrial flares, are very sensitive to crosswinds, such that their combustion efficiencies may decrease sharply below 90% for crosswind speeds above 1 m/sec. Castineira and Edgar[36] also found that excess steam can significantly decrease flare combustion efficiency, perhaps leading to large emissions of HRVOCs. Under such conditions, large emissions of HCHO might also occur. Investigators on the Baylor Aztec in fact saw a "dirty" flare during its morning flight on August 31, 2006, when plumes of apparently primary HCHO were observed on the aircraft. The ratio of HCHO to CO in the plume associated with the flare was found to be 2.3% (Rappenglück et al.[33]).

Another potential underestimated source of HCHO is motor vehicles. Although mobile source emissions inventories do account for primary HCHO, there is some uncertainty in the amount of HCHO that may be attributed to this source category. An in-depth review of diesel exhaust speciation studies from 1991 to 2000 concluded that diesel exhaust had a characteristic HCHO-to-CO ratio of approximately 4%.[37] A follow-up study aimed at improving the limited amount of existing speciation measurements for light-duty diesels arrived within 0.5% of the same ratio.[38] Since 2000, additional speciation studies of diesel emissions have indicated HCHO-to-CO emission ratios that range from 1 to 2.7%.[39–44] These studies included exhaust VOC characterizations for 1974–2000 international and domestic vehicles with multiple fuel blends including oxygenated and nonoxygenated diesel. Although there is a consensus that HCHO-to-CO ratios are higher for diesel than for gasoline vehicles, the literature suggests that HCHO emissions from diesel vehicles remain highly variable.

In addition to being emitted from flares and motor vehicles, HCHO may also be emitted from petrochemical plants as part of a production process, such as in polymer fabrication facilities. However, data to evaluate this possibility are lacking.

An analysis of HCHO-CO relationships based on all in situ measurements at Moody Tower during TexAQS II was conducted by the Rappenglück et al.[33] The analysis discriminated by wind sector between air masses originating from urban areas in Houston and those originating from the Ship Channel. The dataset was also split into night (including rush hour) and daytime measurements. It was discovered that the strongest correlation between HCHO and CO was for urban air masses at night, with a slope of approximately 7 $\text{pptv} \cdot \text{ppbv}^{-1}$, indicating a likely HCHO-to-CO ratio of 0.7% for mobile sources. During the daytime, urban and Ship Channel air masses were found to have weaker correlations, probably because of secondary formation. Interestingly, the HCHO-to-CO slope was greatest for daytime Ship Channel air masses, at approximately 1.7%, similar to the HCHO-to-CO ratio from the analysis of the Baylor Aztec data for the morning of August 31, 2006.

Potential Impact of Increased HCHO. Vizuete et al.[45] performed sensitivity studies with the CAMx three-dimensional (3-D) air quality model used in the Houston SIP to investigate the potential impact of increased primary HCHO on O_3 in the Houston region. They examined two scenarios within the standard 2000 episode coinciding with a portion of the TexAQS I observation period: the first assumed flares to be the source of primary HCHO, and the second assumed additional HCHO is emitted from motor vehicles.

In the first scenario, it was assumed that 1% of the flow from each of 13 flares in the Houston Ship Channel was HCHO that survived the combustion process. In the second scenario, HCHO emissions from low-level sources, which are dominated by motor vehicles, were elevated to 4% of the corresponding CO emissions. (The HCHO added to the inventory was used to measure the sensitivity of O_3 formation and is not a suggested "fix" to motor vehicle emission composition profiles.) Both scenarios resulted in peak O_3 increases of more than 20 ppb relative to the base case with the standard SIP emissions inventory. The results of the flare scenario are shown in Figure 9. Figure 9a shows simulated increases in peak O_3 at monitoring sites of approximately 30 ppb at some locations. Figure 9b shows the spatial variation of the O_3 increases. The largest changes in O_3 concentration were seen immediately at the imputed flares, where HCHO emissions were increased. These enhancements followed

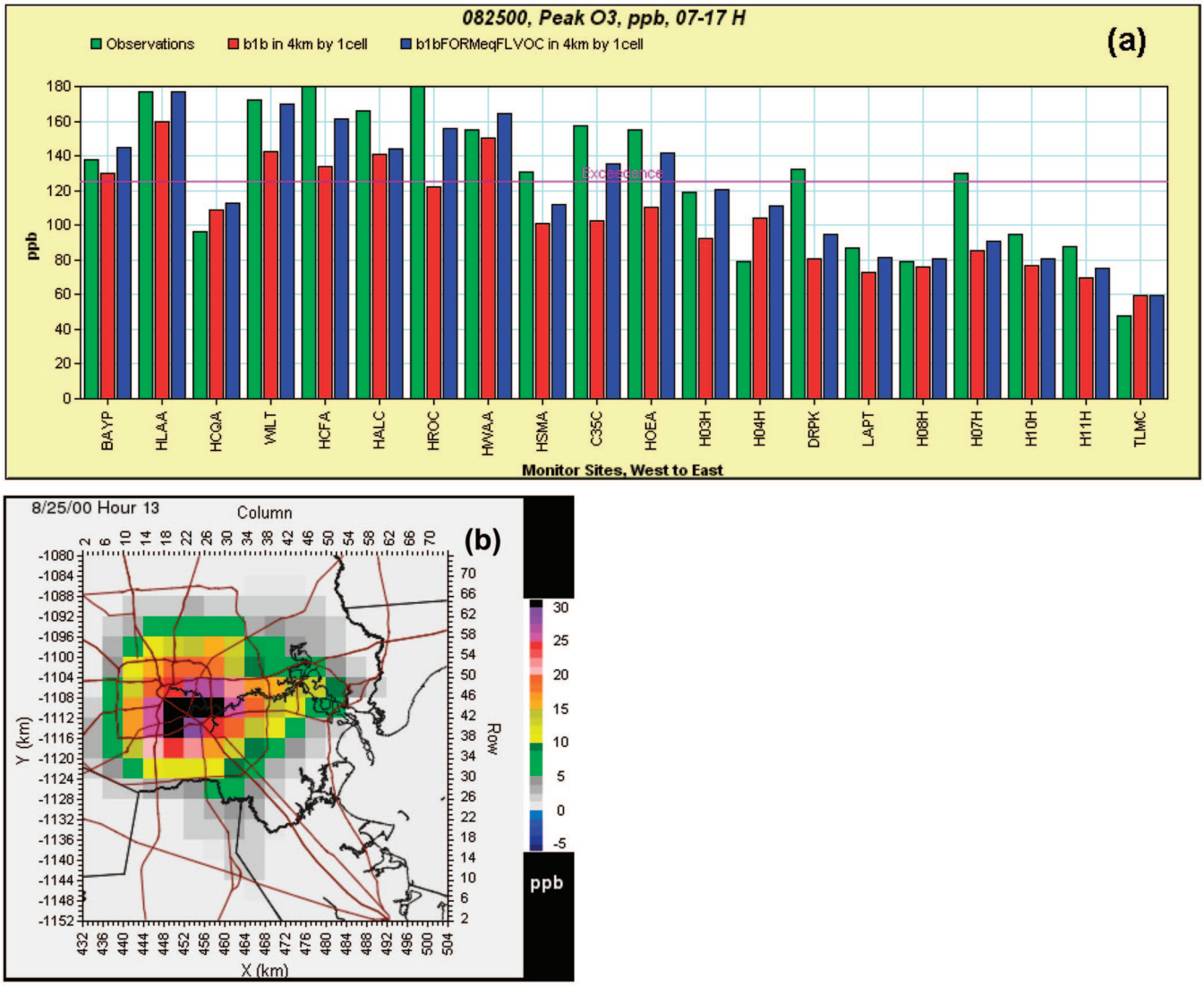

Figure 9. (a) Plot of observed and modeled peak O_3 concentrations for 20 monitors in Houston on August 25, 2000. The base-case simulation using the standard SIP model inventory is denoted by b1b, whereas the sensitivity run incorporating additional emissions of HCHO from flares is denoted by b1bFORMeqFLVOC. Modified with permission from Vizuete et al.[45] Copyright 2006 TERC. (b) Predicted O_3 concentration differences in layer one for 1:00 p.m. central standard time on August 25, 2000 between runs b1bFORMeqFLVOC and b1b.

the O_3 plume as it traveled northwest out of the modeling domain.

It is clear from the results of Vizuete et al.[45] that additional sources of HCHO have the potential to considerably boost O_3 production in Houston, even if OH-driven secondary formation dominates these sources. The preliminary results of TexAQS II suggest that unusual primary or secondary sources of HCHO may indeed have contributed significantly to O_3 formation. The peaks in O_3 above 120 ppb observed to occur at Moody Tower on August 31, 2006 and September 14, 2006 were preceded by mid- to late-morning peaks in HCHO above 15 ppb. The wind on both of these days was northeasterly, which is coming from the direction of the Ship Channel. Moreover, there were large concentrations of SO_2 (>15 ppb) detected during mid- or late morning, suggesting the influence of industrial activities typical of the Ship Channel, such as refining and electrical generation by individual facilities. Continued analysis is required to definitively establish the extent to which emissions of HCHO are underrepresented in current inventories and their contribution to O_3 exceedances in Houston.

HONO

Origin of HONO. HONO from motor vehicle exhaust at night has long been suspected to be a significant source of radicals shortly after sunrise, which may in turn "jump start" photochemical smog formation. A summary of published HONO measurements up to the mid-1990s by Lammel and Cape[46] shows that nocturnal concentrations of HONO in urban areas such as Los Angeles and Milan can exceed 10 ppb. However, such large concentrations cannot be exclusively attributed to mobile sources. Measurements in Caldecott Tunnel indicate ratios of HONO to NO_x in automotive exhaust of approximately 0.3%, with uncertainty arising from possible heterogeneous reactions on tunnel walls (Kirchstetter et al.[47]). Although higher ratios of approximately 0.8% have been reported

in Europe (e.g., Kleffman et al.[48]), primary emissions from motor vehicles alone would not be able to explain observed HONO-to-NO_x ratios in the urban atmosphere of up to several percent (Lammel and Cape[46]).

It is now strongly believed that multiphase reactions on various surfaces yield significant amounts of HONO throughout the entire day (e.g., Alicke et al.[49]). Such multiphase reactions might take place on soil or manmade surfaces, such as buildings and roadways, or on atmospheric particulates. For example, it has been proposed that heterogeneous reactions between NO and HNO_3 adsorbed on surfaces may contribute to "renoxification" of the atmosphere through the production of HONO. Whereas experiments conducted by Kleffmann et al.[50] on glass surfaces in the dark did not produce a significant amount of HONO, a study by Zhou et al.[51] showed HONO production on a sunlit glass manifold.

Gutzwiller et al.[52] suggested that semi-volatile and/or water-soluble species contained in diesel exhaust, but not associated with soot, are significantly involved in secondary HONO formation. To mimic the effects of typical surfaces to which diesel exhaust might be exposed, they performed experiments in which filtered but hot diesel exhaust gas was allowed to interact with water film and dry glass. They found that 2.3% of the NO_x emitted was heterogeneously converted to HONO, at least three times more than the primary HONO emitted by diesel engines.

Stemmler et al.[53] studied the possible daytime conversion of NO_2 to HONO using humic acid films irradiated in the UV-A through the visible spectral regions. They also found evidence for such conversion occurring in the dark, perhaps involving surfaces containing partly oxidized aromatics. These surfaces are ubiquitous. For example, Lam et al.[54] found that aromatic compounds constituted approximately 20% of the organic films coating windows in downtown Toronto. Soil or manmade surfaces exposed to diesel exhaust in the presence of high NO_2 levels may thus be conducive to HONO formation. Stemmler et al.[53] found that photolysis of HONO formed on surfaces could account for up to 60% of the integrated source of OH radicals in the lower boundary layer.

Heterogeneous formation of HONO may not be limited to the urban canopy. Ammann et al.[55] reported the efficient conversion of NO_2 to HONO on fresh soot particles in the presence of water. They suggested that interaction between NO_2 and soot particles may account for high mixing ratios of HONO observed in urban environments. However, the kinetic details of this process have not yet been successfully elucidated, although it is generally agreed that the relevant conversion reaction has a linear dependence on NO_2.[56]

Bröske et al.[57] considered the possibility that heterogeneous conversion of NO_2 on secondary organic aerosol (SOA) may generate HONO. They used reactions of O_3 and OH with various aromatics to produce different organic aerosols, which were then sampled on filters and exposed to humidified NO_2 mixtures. The HONO formation rates observed by Bröske et al.[57] were too low for them to conclude that SOA could be a significant substrate for heterogeneous HONO formation. More recently, Stemmler et al.[58] investigated reactions of gaseous NO_2 with aerosols consisting of humic acids under different light conditions in aerosol flow tube experiments. Although such reactions did indeed produce HONO, they concluded that ground-level humic materials would have a much larger impact on HONO formation than humic materials on airborne particles.

Observational evidence on the relative importance of the Earth's surface and atmospheric particulate matter in mediating HONO formation is somewhat equivocal. Evidence for the involvement of both surface types had been found from field studies well before 2000, such as correlations between HONO and radon (which originates exclusively from the ground) and between HONO and particulate matter surface area (Lammel and Cape[46]).

Reisinger[59] made DOAS measurements of HONO, NO_2, and aerosol surface density during winter in Christchurch, New Zealand. He found HONO concentrations to be correlated with those of NO_2, with the highest HONO values occurring at night when particulate matter levels were also high. In addition, Reisinger[59] deduced a strong correlation between the HONO-to-NO_2 ratio and aerosol surface density, suggesting that significant heterogeneous formation of HONO may occur through reactions of NO_2 on aerosol surfaces.

An interesting contrast to the study of Reisinger[59] was provided by Kleffman et al.,[48] who conducted nocturnal measurements of HONO using long-path absorption photometry (LOPAP), along with measurements of NO, NO_2, and vertical gradients in particulate matter area density on a research tower in a semi-rural area in Germany. They found that below 100 m the HONO-to-NO_2 ratio decreased with increasing altitude, whereas the particle surface area density was roughly constant so that there was no correlation between these two quantities. Kleffman et al.[48] concluded that nighttime HONO formation was dominated by processes on ground surfaces and that significant HONO formation on particles could be excluded at their particular measurement site. In addition to their nocturnal gradient measurements, Kleffman et al.[48] observed high daytime HONO concentrations at constant altitude, which pointed to a significant and yet unknown daytime source of HONO.

In a review of relevant HONO measurements, Kleffman,[60] postulated the existence of a missing volume source during the day, such as a photochemical gas- or particle-phase formation mechanism. Candidate heterogeneous mechanisms for the missing volume source of HONO include (1) photolysis of adsorbed NO_3, HNO_3, organic nitrates, or other nitrogen compounds; and (2) reduction of HNO_3 to HONO by photosensitized organic impurities.[60] Recent research has also uncovered possible new gas-phase HONO formation mechanisms involving the photolysis of ortho-nitrophenols and methyl-substituted nitroaromatics resulting from the decomposition of primary aromatics in the urban atmosphere.[60,61] Lastly, HONO as well as OH may be generated in the gas phase through reactions between excited states of NO_2 and water vapor.[12]

Evidence of Additional HONO Production from TexAQS II. TRAMP provided a rich dataset with which to investigate the origin of HONO, whether from primary emissions or from secondary formation. Figure 10 summarizes the

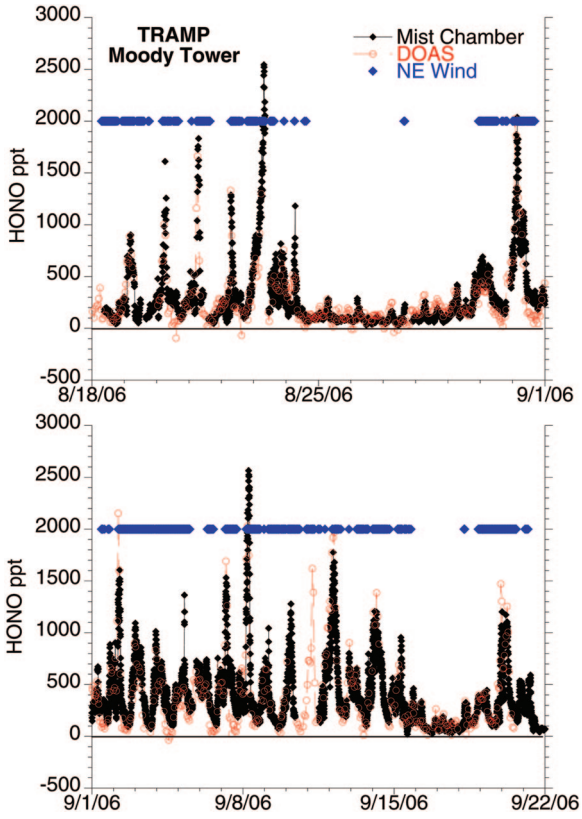

Figure 10. Overview of the TRAMP HONO dataset as measured by mist chamber/IC (black points) and the lower light path of the long-path DOAS instrument (red points). Periods of northeasterly winds are identified by blue symbols at the top of the graphs. Modified with permission from Stutz et al.[28] Copyright 2009 *Atmospheric Environment*, Elsevier.

TRAMP HONO dataset as measured by IC and the lower path of the long-path DOAS instrument. Note the tendency of large HONO peaks to coincide with periods of northeasterly flow from the Ship Channel. The TRAMP IC and DOAS measurements of HONO are broadly consistent with each other. However, significant differences in daytime HONO mixing ratios were apparent on a few days of the experiment. These days all showed the characteristics of heavy pollution episodes under the influence of winds from the northeast (355° to 120°) for most of the 9:00 a.m. to 3:00 p.m. period. However, there were several other days with midday winds from this sector that had small, or even no, discrepancy between the HONO measurements. Stutz et al.[28] deduced that the positive daytime bias of the IC instrument during a few days is positively correlated with photochemically produced compounds such as O_3, HNO_3, and HCHO, but not with NO_2, NO_x, HNO_4, or the NO_2 photolysis rate. Although an interferant could not be identified, organic nitrites appear a possible explanation for these observations.

Observed HONO concentrations during TexAQS II varied considerably from a minimum of 100–200 ppt around sunset to above 2 ppb at night or during morning rush hour. Sometimes HONO remained above 500 ppt almost the entire morning, such as on September 14, 2006. By comparison, daytime HONO levels observed with the DOAS technique during the BERLIOZ campaign never exceeded the detection limit of approximately 110 ppt, except during the early morning, with maximum values of approximately 1.1 ppb occurring just before sunrise (Alicke et al.[19]). Stutz et al.[21] likewise reported HONO concentrations of approximately 1 ppb at La Porte in Houston throughout the early morning of September 5, 2000 during TexAQS I. On the other hand, Acker et al.[62] reported up to 2 ppb of HONO accumulated during the night, with unexpectedly high HONO concentrations of several hundred ppt during the day during the Nitrous Acid and its Influence on the Oxidation Capacity of the Atmosphere experiment (NITROCAT) in Rome, Italy, during May and June of 2001. In that study, HONO was measured using DOAS and in situ wet collection techniques.

Photolysis acts as a very strong sink of HONO, so sustained mixing ratios of several hundred ppt observed during TRAMP on some days indicate continuous production from enhanced levels of nitrogenous species in Houston. The observed HONO mixing ratios are more than can be explained by homogeneous gas-phase chemistry alone as currently simulated in SIP air quality models, which do not predict HONO concentrations above 100 ppt. Larger HONO concentrations observed after sunset are due to shutdown of the photolytic sink and a possible nighttime source. The DOAS observations consistently show a vertical gradient of HONO at night and in the early morning, with smaller concentrations aloft, consistent with the results of Kleffman et al.[48] This indicates a surface source in either traffic or the urban canopy.

When the HONO data are examined in the context of other observations, some interesting features emerge. Nocturnal peaks in HONO appear to coincide with high concentrations of HO_x. Bursts of NO_x, as during morning rush hour, are also clearly conducive to high HONO concentrations. In addition, peaks in HONO are usually linked with high concentrations of organic and/or NO_3 aerosol, indicating the heterogeneous formation of HONO on aerosols or the correlation between increasing organic aerosol and some other source of HONO, such as emission or secondary production at the ground. Moreover, there is sometimes a noticeable anticorrelation between HONO and HNO_3 as confirmed by Ziemba et al.,[63] who explored the possible formation of HONO from heterogeneous reactions involving HNO_3.

On the basis of the TRAMP data, Ziemba et al.[63] hypothesized a nonphotolytic mechanism of secondary HONO formation. They found that during early morning rush hour HONO is strongly correlated with aerosol surface area, and that rush hour organic aerosol is less oxidized and more similar to hydrocarbon-like organic aerosol (HOA). Coinciding elevated CO and acetylene concentrations indicate that HOA is primary in nature and closely related to vehicular emissions. Ziemba et al.[63] computed the excess amount of observed HONO over a theoretical amount associated with known formation mechanisms and found that this excess HONO was strongly correlated with HNO_3. They therefore concluded that HONO was secondarily formed by heterogeneous conversion of HNO_3 on HOA associated with

traffic emissions. Although Ziemba et al.[63] could not identify an explicit detailed mechanism for this process, they noted that several polyaromatic hydrocarbon compounds were enriched during HONO events, suggesting their importance for HNO_3 conversion.

Although the hypothesis of Ziemba et al.[63] may explain bursts of HONO during morning rush hour, it does not explain why high concentrations of HONO are associated with flow from the Houston Ship Channel. A more speculative hypothesis is currently being investigated in which substrate for heterogeneous HONO formation may be derived from any aerosol-phase organic NO_3 byproducts from nocturnal reactions of NO_3 radical with industrial emissions of olefins such as isoprene and 1,3-butadiene. According to the analysis of TRAMP data by Stutz et al.[64] these compounds dominate the nocturnal chemistry of NO_3 in Houston, unlike in other urban areas. The alternative hypothesis for HONO formation involving organic nitrates is made more intriguing by the analysis of measurements of total and speciated reactive nitrogen during TRAMP by Luke et al.,[65] who concluded that there is a ubiquitous unknown reactive nitrogen reservoir compound present in the nocturnal Houston atmosphere.

Potential Impacts of Increased HONO. The persistence of HONO concentrations of the order of 1 ppb well beyond the early morning has the potential to affect peak O_3 through the production of radicals. Mao et al.[66] examined the radical budget in Houston during TexAQS I and TexAQS II on the basis of corresponding field observations and found that HONO played a more prominent role in the HO_x budget during TexAQS II compared with TexAQS I. Their analysis of TRAMP data revealed that HONO was the largest source of HO_x from early to mid-morning during the 2006 study. (They also found that the contribution of HCHO to HO_x was similar in magnitude to that of $H_2O + O(^1D)$ during the entire TRAMP experiment.)

The University of Houston[67] performed simulations of radical chemistry at Moody Tower without observational constraints on HONO for the time period August 18 through September 30, 2006 using a box model equipped with the Regional Atmospheric Chemistry Modeling[68] (RACM) mechanism. The model had 77 chemical species and 237 gas-phase reactions with rate coefficients updated according to Sander et al.[69] Model input and output were as follows:

Model input

- Inorganic gases: O_3, NO, NO_2, CO, SO_2, H_2O_2, and HNO_3
- VOC species: Non-methane hydrocarbons (GC-FID), HCHO (Hantzsch), and other oxygenated hydrocarbons as measured by protein transfer reaction (PTR)-mass spectrometry (MS)
- Photolysis rates: Scaled to measurements or calculated with the tropospheric UV and visible (TUV) radiation algorithm[70]
- Meteorological parameters: Temperature, pressure, and relative humidity (RH)

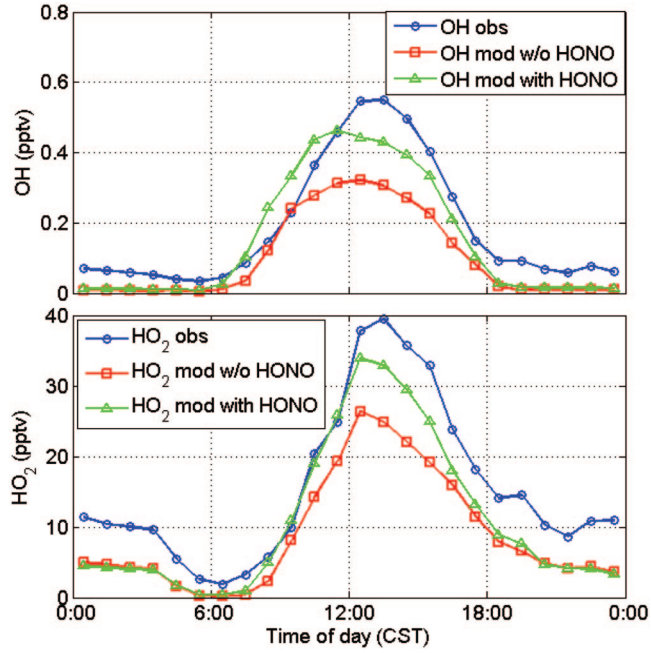

Figure 11. Observations and box model simulations of HO_x radical concentrations during TRAMP. Model results are shown for two cases: (1) without any HONO, and (2) with HONO constrained by TRAMP observations.

Model output

- Steady-state OH, HO_2, organic peroxy radicals (RO_2), and other intermediates.

Initial RACM box model analyses by the University of Houston[67] were performed before the HONO observations from TRAMP were available. These analyses have since been repeated with the new HONO data as input.

Figure 11 compares HO_x concentrations measured during TRAMP with predictions from the RACM box model including HCHO constrained by TRAMP observations but without any HONO. Overall, observed and modeled HO_x follow the same typical diurnal variation; however, the model underpredicts HO_x during the day and at night. This underprediction may be due to measurement errors, missing OH sources, or incomplete chemistry in the model. On average, daytime OH and HO_2 are both underpredicted by about a factor of 2. Figure 11 also shows box model results from a simulation in which HONO was constrained by TRAMP observations. The simulation of daytime HO_x is significantly improved by including HO_x produced from the photolysis of HONO, although it does not completely overcome the problem of HO_x underprediction.

The underprediction of HO_x is not unique to the TRAMP experiment or the RACM chemical mechanism. For comparison, observed daytime concentrations of OH and HO_2 during the SOS campaign were generally a factor of 1.33 and 1.56 times those of box model-predicted values (Martinez et al.[19]). Similarly, Chen et al.[71] performed box model simulations using TRAMP data and various gas-phase chemical mechanisms and found that OH and HO_2 were generally underpredicted by all mechanisms, even when HONO was constrained by observations.

The increased production of HONO from heterogeneous reactions on various surfaces may accelerate the

nonlinear chemistry of O_3. Lei et al.[72] performed a 3-D modeling study of O_3 formation in the Houston region for a 1993 O_3 episode. They conducted several sensitivity experiments, including one in which heterogeneous conversion of NO_2 to HONO was assumed to occur on soot surfaces. Lei et al.[72] found that this heterogeneous conversion accelerated O_3 production by approximately 1 hr in the morning and led to an increase in daytime O_3 of up to 12 ppb.

Very recently, Sarwar et al.[73] performed a model sensitivity study using the 3-D Community Multiscale Air Quality (CMAQ) model, in which the model performance against observations from the 2001 Northeast Oxidant and Particle Study was compared for four different cases: (A) standard CMAQ emissions; (B) emissions from case A plus HONO emissions; (C) emissions from case B plus heterogeneous HONO formation from reaction of NO_2 and H_2O on urban canopy and particulate matter surfaces; and (D) emissions and chemistry from case C plus a surface photolytic source of HONO involving conversion of adsorbed HNO_3. They found a progressive improvement in the model performance as additional sources of HONO were added. Sarwar et al.[73] concluded that (1) emissions and gas-phase reactions are relatively minor sources of HONO, (2) heterogeneous reaction is the most significant source of HONO at night, and (3) surface photolysis is the most significant source of HONO during the day.

NIGHTTIME RADICAL SOURCES

Considerable attention is paid in SIP modeling to daytime photochemistry. However, nighttime chemistry is the subject of increasing research because of the potential sequestration of NO_x in nocturnal reservoirs and the formation of radicals that may fuel O_3 photochemistry after sunrise. The main starting point for atmospheric chemistry in the absence of solar radiation is the conversion of NO first to NO_2 and then to NO_3 in reactions involving O_3. NO_3 may either react with NO_2 or a suite of VOCs including aldehydes, short-lived alkenes, and fast-reacting terpenes. This way nitrogen compounds can be removed through formation of HNO_3 on particles or nocturnal radicals can be produced.

An alternative route to the formation of nighttime radicals is the reaction of O_3 with olefins. Kanaya et al.[74] made nighttime LIF measurements of HO_2 radical under relatively clean conditions at Oki Island, Japan. They found unexpectedly large concentrations of HO_2 of approximately 3 ppt. Kanaya et al.[74] then performed model calculations constrained by ancillary measurements. These calculations indicated that HO_2 under clean conditions was produced primarily via the reactions of O_3 with olefins and that NO_3 chemistry was relatively unimportant.

Geyer et al.[75] used a photochemical box model to study the role of NO_3 and other trace gases in the nighttime budget of radicals during the BERLIOZ campaign, when HO_2 mixing ratios of up to 4 ppt and OH concentrations of up to 1.8×10^5 molecules cm^{-3} were observed. They showed that nocturnal reactions of NO_3 with VOCs (mainly biogenic monoterpenes) constituted a considerable source of RO_2. Geyer et al.[75] also calculated campaign-averaged contributions of NO_3 to the nighttime production of OH and HO_2 of 36 and 53%, respectively, the rest of the production of these radicals being due to nighttime ozonolysis.

During TRAMP, significant nighttime HO_2 and OH levels were frequently measured, especially when nighttime O_3 levels were high. Over 25 ppt of HO_2 and 0.1 ppt of OH were observed at approximately 12:00 a.m. on September 14, 2006 when O_3 exceeded 40 ppb (see Figures 6 and 7). On the night of September 6–7, 2006 O_3 concentrations were as large as 60–80 ppb, when up to 40 ppt of HO_2 and 0.4 ppt of OH were detected. The peak nighttime HO_2 concentrations measured during TRAMP are an order of magnitude greater than concentrations observed during BERLIOZ and SOS (~4 ppt).[20,75] The median nighttime OH concentration measured during TRAMP was approximately 0.05 ppt, which is approximately 10^6 molecules/cm^3, similar to the average nighttime OH concentration observed during the SOS campaign (Martinez et al.[20]) but still several times larger than the peak concentrations observed during BERLIOZ.

Whether there is any connection between high concentrations of HO_2 at night and subsequent daytime O_3 production is unclear. TRAMP observations indicate that HO_2 mixing ratios can drop precipitously before dawn (see Figures 3 and 7), possibly because of liquid partitioning of HO_2 reservoirs such as H_2O_2 and HNO_4 as the RH approaches 100%. Interestingly, the decline in HO_2 is typically followed by a rapid rise in HONO.

The dissolution of gaseous HONO and HNO_4 in aqueous droplets results in the presence of nitrite ions in dew. Rubio et al.[76] measured concentrations of cations and anions in rain and dew in Santiago, Chile, from 1995 to 1999. They found that dew had relatively large nitrite concentrations of up to 180 μeq/L. Rubio et al.[76] suggested that such large levels of dew nitrite could produce significant gaseous HONO in the early morning when droplets evaporate, possibly through the decomposition of ammonium nitrite.

A potential mechanism for conversion of HO_x into HONO involves HNO_4. Like HONO, HNO_4 has generally been neglected as a source of radicals in air quality models used in SIP applications. However, Geyer and Stutz[77] studied the role of vertical structure and transport in the formation of nighttime radicals using an idealized one-dimensional model and concluded that HNO_4 plays a significant role in producing HO_x at the surface. They found that a positive nocturnal vertical gradient of HNO_4 is formed through the destruction of HO_2 by NO near the ground. This gradient then leads to a downward transport of HNO_4 followed by its thermal decomposition to produce HO_x.

Dentener et al.[78] suggested that the aqueous-phase reaction of HNO_4 exerts a significant influence on tropospheric chemistry. Motivated by this, Williams et al.[79] deployed a one-dimensional marine stratocumulus cloud model supplemented with an aqueous-phase chemical mechanism to assess the impact of clouds and aerosols on gas-phase HO_x, NO_x, and O_3 in the marine boundary layer. They found that clouds may act as a heterogeneous source of gaseous HONO via the conversion of HNO_4 at moderate pH (~4.5).

Kim et al.[80] made direct in situ measurements of HNO_4 in the upper troposphere using chemical ionization mass spectrometry (CIMS) during the Intercontinental Chemical Transport Experiment—North America 2004. They found a maximum volume mixing ratio of 76 ppt at an altitude of 8–9 km. One would normally expect much smaller values than this in the boundary layer because of warmer temperatures and increased thermal decomposition, but the large nocturnal concentrations of HO_2 and NO_2 observed during TRAMP point to the possibility of unusually large concentrations of HNO_4 at night in Houston.

Using typical nocturnal concentrations for HO_2 (20 ppt) and NO_2 (17 ppb) observed during TRAMP and assuming an equilibrium constant for HNO_4 of 1.9×10^{-11} cm^3 corresponding to a temperature of 23.5 °C, on the basis of the recommendation of Sander et al.[69] the authors estimate an equilibrium concentration of approximately 165 ppt for HNO_4. Constrained box model calculations confirm that concentrations of HNO_4 between 150 and 200 ppt may indeed have occurred on some nights during the TRAMP study.

Significant nocturnal concentrations of HNO_4 may be conducive to a night-to-morning transition mechanism by which nighttime and early morning radicals may influence daytime O_3 to a non-negligible degree. During the night, HNO_4 acts as a HO_x reservoir aloft and a HO_x source near the ground. At dawn, the rise in RH turns HNO_4 into a HO_x sink. Dissolved HNO_4 is converted in dew, clouds, or aerosols into HONO, which then acts as a HO_x source in the morning. This process could be aided by the coastal influence on Houston, which could limit the acidity of potential substrates despite the presence of large pollution sources.

Regardless of their ultimate fate, the peak concentrations of nighttime radicals observed during TRAMP are considerably larger than anticipated from previous measurements or box model calculations. Future measurements and analyses will explore whether O_3-olefin or NO_3-olefin reactions are required to explain these large values and their implications for O_3 productivity in Houston during the day.

CONCLUSIONS

TERC-funded projects during TexAQS II yielded surprising new information that may help to improve O_3 SIP modeling for Houston. Preliminary results indicate the possible importance of underestimated primary and/or secondary HCHO and HONO, two important radical reservoirs that may substantially increase the production of O_3. Undercounted primary sources of HCHO may include flares, motor vehicles, and polymer fabrication facilities, whereas nocturnal and daytime reactions between O_3 and industrial olefins may lead to significant secondary production of HCHO. Sources of HONO include multiphase reactions on aerosols, soot, soil, and manmade surfaces. In addition, reactions of O_3 and NO_3 with olefins may contribute to observed high concentrations of radicals at night, although the implications of these concentrations for subsequent daytime O_3 production are unknown. HNO_4 may serve as a temporary nocturnal reservoir of radicals and an early morning source of HONO. On the other hand, conversion of HNO_3 to HONO may take place on organic aerosol from rush hour traffic emissions. More speculatively, aerosol formed from organic NO_3 byproducts of nocturnal reactions between the NO_3 radical and industrial olefins may serve as an additional substrate for HONO formation.

The enhancement of radical sources in the SIP model may better enable the State of Texas to demonstrate attainment of the 8-hr O_3 standard in Houston by increasing the simulated effectiveness of current control strategies. The imposition of future controls on radical precursors may further improve Texas' ability to attain the standard. However, considerable work remains to be done to prove these hypotheses. Future research tasks include (1) the determination of the relative importance of primary versus secondary HCHO in Houston, (2) the quantification of HCHO emissions from flares and polymer fabrication facilities, (3) new laboratory and field measurements of heterogeneous formation mechanisms for HONO and their eventual inclusion in SIP models, and (4) further investigation of the role of nighttime radical formation in subsequent daytime O_3 formation.

ACKNOWLEDGMENTS

Funds for the TexAQS II research projects managed by TERC were provided by the Texas Legislature through TCEQ. The views expressed in this article are those of the individual authors and do not necessarily reflect the views and policies of EPA. This article has been reviewed and approved for presentation and publication by EPA's National Center for Environmental Assessment. N.B. Reports of TERC projects are available at: http://www.tercairquality.org.

REFERENCES

1. Olaguer, E.; Jeffries, H.; Yarwood, G.; Pinto, J. Attaining the 8-hr Ozone Standard in East Texas; *EM* **2006**, *October*, 26-29.
2. Daum, P.H.; Kleinman, L.I.; Springston, S.R.; Nunnermacker, L.J.; Lee, Y.-N.; Weinstein-Lloyd, J.; Zheng, J.; Berkowitz, C. A Comparative Study of O_3 Formation in the Houston Urban and Industrial Plumes during the TEXAQS 2000 Study; *J. Geophys. Res.* **2003**, *108*; doi: 10.1029/2003JD003552.
3. Cowling, E.B.; Furiness, C.; Dimitriades, B.; Parrish, D. *Final Rapid Science Synthesis Report: Findings from the Second Texas Air Quality Study (TexAQS II), Report to the Texas Commission on Environmental Quality*; North Carolina State University: Raleigh, NC, 2007.
4. Nielsen-Gammon, J. *Project H-45-D-2005 TAMU (582-4-65587), Final Report*; Texas Environmental Research Consortium: Houston, TX, 2006.
5. Byun, D.; Kim, S.; Jang, M.; In, H.; Song, C.-K.; Perna, R.; Cheng, F.-Y.; Ngan, F.; Percell, P.; Hamilton, W.; Ningthoujam, S.; Ho, T.; Lin, J.; Seigneur, C.; Pun, B.; Stockwell, W. *Modeling Strategy in Support of TexAQS-II and 8-Hour Ozone Assessment, HARC Project H45 Interim Report for Task Group A*; Institute for Multidimensional Air Quality Studies; Texas Environmental Research Consortium: Houston, TX, 2005.
6. *TEXAQS/GoMACCS Science and Implementation Plan March 2005*; National Oceanic and Atmospheric Administration: Washington, DC, 2006.
7. Mellqvist, J.; Samuelsson, J.; Rivera, C.; Lefer, B.; Patel, M. *Measurements of Industrial Emissions of VOCs, NH_3, NO_2 and SO_2 in Texas Using the Solar Occultation Flux Method and Mobile DOAS, Project H53 Final Report*; Texas Environmental Research Consortium: Houston, TX, 2007.
8. Berkowitz, C.; Alexander, M.L.; Yu, X.-Y.; Ortega, J.; Jobson, T. *The Houston Triangle, Project H75 Final Report*; Texas Environmental Research Consortium: Houston, TX, 2006.
9. University of Houston. *TexAQS II Radical Measurement Project (TRAMP), Project H78 Final Report*; Texas Environmental Research Consortium: Houston, TX, 2007.
10. Alvarez, S.; Kauffman, L.; Compton, T.; Zanin, G.; Shauck, M.; Buhr, M. *H-63 Aircraft Measurements in Support of TexAQS II, Project H63 Final*

Report; Texas Environmental Research Consortium: Houston, TX, 2007.
11. Lefer B.; Rappenglück B.; Flynn, J.; Haman, C. Photochemical and Meteorological Relationships during the TexAQS-II Radical and Aerosol Measurement Project (TRAMP); *Atmos. Environ.,* submitted for publication.
12. Li, S.; Matthews, J.; Sinha, A. Atmospheric Hydroxyl Radical Production from Electronically Excited NO_2 and H_2O; *Science* **2008**, *319,* 1657-1660.
13. Jeffries, H.; Kim, B.-U.; Jobes, D.; Pennington, E.; Arunachlam, S.; Eyth, A.; Adelmon, Z.; Holland, A.; Pai, P.; Partheepan, P.; Schwede, B.; Vukovich, J. *Role of Modeling Assumptions in the Houston Mid-Course Review, Project H12.8HRB, Final Report*; Prepared by the University of North Carolina at Chapel Hill for the Texas Environmental Research Consortium: Houston, TX, 2005.
14. Vizuete, W.; Jeffries, H.; Christoph, E.; Henderson, B.; Parikh, H.; Valencia, A. *Multi-resolution Simulation and Analysis of TexAQS II Air Pollution Events, H87 Final Report*; Prepared by the University of North Carolina–Chapel Hill for the Texas Environmental Research Consortium: Houston, TX, 2007.
15. Allen, D.; Murphy, C.; Kimura, Y.; Vizuete, W.; Edgar, T.; Jeffries, H.; Kim, B.-U.; Webster, M.; Symons, M. *Variable Industrial VOC Emissions and their Impact on Ozone Formation in the Houston-Galveston Area, Project H13 Final Report*; Texas Environmental Research Consortium: Houston, TX, 2004.
16. Ryerson, T. B.; Trainer, M.; Angevine, W.M.; Brock, C.A.; Dissly, R.W.; Fehsenfeld, F.C.; Frost, G.J.; Goldan, P.D.; Holloway, J.S.; Hübler, G.; Jakoubek, R.O.; Kuster, W.C.; Neuman, J.A.; Nicks, D.K., Jr.; Parrish, D.D.; Roberts, J.M.; Sueper, D.T.; Atlas, E.L.; Donnelly, S.G.; Flocke, F.; Fried, A.; Potter, W.T.; Schauffler, S.; Stroud, V.; Weinheimer, A.J.; Wert, B.P.; Wiedinmyer, C.; Alvarez, R.J.; Banta, R.M. Darby, L.S.; Senff, C.J. Effect of Petrochemical Industrial Emissions of Reactive Alkenes and NO_x on Tropospheric Ozone Formation in Houston, Texas; *J. Geophys. Res.* **2003**, *108*, doi: 10.1029/2002JD003070.
17. Banta, R. M.; Senff, C.J.; Nielsen-Gammon, J.; Darby, L.S.; Ryerson, T.B.; Alvarez, R.J.; Sanberg, S.P.; Williams, E.J.; Trainer, M. A Bad Air Day in Houston; *Bull. Am. Meteorol. Soc.* **2005**, *86*, 657-669.
18. Platt, U.; Alicke, B.; Dubois, R.; Geyer, A.; Hofzumahaus, A.; Holland, F.; Martinez, M.; Mihelcic, D.; Klupfel, T. Lohrmann, B.; Pätz, W.; Perner, D.; Rohrer, F.; Schäfer, J.; Stutz, J. Free Radicals and Fast Photochemistry during BERLIOZ; *J. Atmos. Chem.* **2002**, *42,* 359-394.
19. Alicke, B.; Geyer, A.; Hofzumahaus, A.; Holland, F.; Konrad, S.; Pätz, H. W.; Schäfer, J.; Stutz, J.; Volz-Thomas, A.; Platt, U. OH Formation by HONO Photolysis during the BERLIOZ Experiment; *J. Geophys. Res.* **2003**, *108*, doi: 10.1029/2001JD000579.
20. Martinez, M.; Harder, H.; Kovacs, T.A.; Simpas, J.B.; Bassis, J.; Lesher, R.; Brune, W.H.; Frost, G.J.; Williams, E.J.; Stroud, C.A.; Jobson, B.T.; Roberts, J.M.; Hall, S.R.; Shetter, R.E.; Wert, B.; Fried, A.; Alicke, B.; Stutz, J.; Young, V.L.; White, A.B.; Zamora, R.J. OH and HO_2 Concentrations, Sources, and Loss Rates during the Southern Oxidants Study in Nashville, Tennessee, Summer 1999; *J. Geophys. Res.* **2003**, *108*, doi: 10.1029/2003JD003551.
21. Stutz, J. B.; Alicke, B.; Ackermann, R.; Geyer, A.; Wang, S.; White, A.B.; Williams, E.J.; Spicer, C.W.; Fast, J.D. Relative Humidity Dependence of HONO Chemistry in Urban Areas; *J. Geophys. Res.* **2004**, *109*, doi: 10.1029/2003JD004135.
22. Matthew, L.; Tai, W.R.; Lo, J.-G. Measurements of Sulfur Dioxide and Formaldehyde in Taipei Using a Differential Optical Absorption Spectrometer; *J. Air & Waste Manage. Assoc.* **2001**, *51,* 94-101.
23. Stutz, J.B.; Alicke, B.; Ackermann, R.; Geyer, A.; White, A.B.; Williams, E.J. Vertical Profiles of NO_3, N_2O_5, O_3, and NO_x in the Nocturnal Boundary Layer: 1. Observations during the Texas Air Quality Study 2000; *J. Geophys. Res.* **2004**, *109*, doi: 10.1029/2003JD004209.
24. Dasgupta, P.; Li, J.Z.; Zhang, G.; Luke, W.; McClenny, W.A.; Stutz, J.; Fried, A. Summertime Ambient Formaldehyde in Five U.S. Metropolitan Areas: Nashville, Atlanta, Houston, Philadelphia, and Tampa; *Environ. Sci. Technol.* **2005**, *39,* 4767-4783.
25. Wert, B.P.; Trainer, M.; Fried, A.; Ryerson, T.B.; Henry, B.; Porter, W. Angevine, W.M.; Atlas, E.; Donnelly, S.G.; Fehsenfeld, F.C.; Frost, G.J.; Goldan, P.D.; Hansel, A.; Holloway, J.S.; Hubler, G.; Kuster, W.C.; Nicks, D.K.; Neuman, J.A.; Parrish, D.D.; Schauffler, S.; Stutz, J.; Sueper, D.T.; Wiedinmyer, C.; Wisthaler, A. Signatures of Terminal Alkene Oxidation in Airborne Formaldehyde Measurements during TexAQS 2000; *J. Geophys. Res.* **2003**, *108*, doi: 10.1029/2002JD002502.
26. Apel, E.C.; Brauers, T.; Koppmann, R.; Bandowe, B.; Bobmeyer, J.; Holzke, C.; Tillmann, R.; Wahner, A. Wegener, R.; Brunner, A.; Jocher, M.; Ruuskanen; Spirig, C.; Steigner, D.; Steinbrecher, R.; Gomez Alvarez, E.; Müller, K.; Burrows, J.P.; Schade, G. Solomon, S.J.; Ladstätter-Weibenmayer, A. Simmonds, P.; Young, D.; Hopkins, J.R.; Lewis, A.C.; Legreid, G.; Reimann, S.; Hansel, A.; Wisthaler, A.; Blake, R.S. Ellis, A.M.; Monks, P.S.; Wyche, K.P. Intercomparison of Oxygenated Volatile Organic Compound (OVOC) Measurements at the SAPHIR Atmosphere Simulation Chamber; *J. Geophys. Res.* **2008**, *113*, doi: 10.1029/2008JD009865.
27. Wisthaler, A.; Apel, E.C. Bossmeyer, J.; Hansel, A.; Junkermann, W.; Koppmann, R.; Meier, R.; Müller, K.; Solomon, S.J.; Steinbrecher, R.; Tillmann, R.; Brauers, T. Intercomparison of Formaldehyde Measurements at the Atmosphere Simulation Chamber SAPHIR; *Atmos. Chem. Phys.* **2008**, *8,* 2189-2200.
28. Stutz, J.; Oh, H.-J.; Whitlow, S.I.; Anderson, C.; Dibb, J.E.; Flynn, J.H.; Rappenglück, B.; Lefer, B. Intercomparison of DOAS and Mist-Chamber IC Measurements of HONO in Houston, TX; *Atmos. Environ.*, in press.
29. Canagaratna, M. R.; Jayne, J.T.; Jimenez, J.L.; Allan, J.D.; Alfarra, M.R. Zhang, Q.; Onasch, T.B.; Drewnick, F.; Coe, H. Middlebrook, A.; Delia, A.; Williams, L.R.; Trimborn, A.M.; Northway, M.J.; DeCarlo, P.F.; Kolb, C.E.; Davidovits, P.; Worsnop, D.R. Chemical and Microphysical Characterization of Ambient Aerosols with the Aerodyne Aerosol Mass Spectrometer; *Mass Spec. Rev.* **2007**, *26,* 185-222.
30. Faloona, I.C.; Tan, D. Lesher, R.L.; Hazen, N.L.; Frame, C.L.; Simpas, J.B.; Harder, H.; Martinez, M.; Di Carlo, P.; Ren, X.; Brune, W.H. A Laser-Induced Fluorescence Instrument for Detecting Tropospheric OH and HO_2: Characteristics and Calibration; *J. Atmos. Chem.* **2004**, *44,* 139-167.
31. Eom, I.-Y.; Li, Q.; Li, J.; Dasgupta, P.K. Robust Hybrid Flow Analyzer for Formaldehyde; *Environ. Sci. Technol.* **2008**, *42,* 1221-1226.
32. Friedfeld, S.; Fraser, M.; Ensor, K.; Tribble, S.; Rehle, D.; Leleux, D.; Tittel, F. Statistical Analysis of Primary and Secondary Atmospheric Formaldehyde; *Atmos. Environ.* **2002**, *36,* 4767-4775.
33. Rappenglück, B.; Byun, D.; Czader, B.; Ki, S.; Leuchner, M.; Alvarez, S.; Kauffman, L.; Shauck, M.; Zanin, G.; Buhr, M.; Dasgupta, P.; Estes, M.; Luke, W. Analysis of Primary vs. Secondary Fraction of Formaldehyde in the Houston Area during TexAQS II. Presented at the 88th Annual Meeting of the American Meteorological Society, 10th Conference on Atmospheric Chemistry, New Orleans, LA, 2008; Paper 1.5.
34. Seebold, J.; Gogoloek, P.; Pohl, J.; Schwartz, R. Practical Implications of Prior Research on Today's Outstanding Flare Emissions Questions and a Research Program to Answer Them. Presented at the AFRC-JFRC 2004 Joint International Combustion Symposium, Maui, HI, October 2004; available at http://www.nrcan.gc.ca/es/etb/cetc/ifc/Pubs/Comb_symp_paper_oct_2004_e.htm (accessed 2009).
35. Castineira, D.; Edgar, T.F. CFD for Simulation of Crosswind on the Efficiency of High Momentum jet Turbulent Combustion Flames; *J. Environ. Eng.* **2008**, *134,* 561-571.
36. Castineira, D.; Edgar, T. F. CFD for Simulation of Steam-Assisted and Air-Assisted Flare Combustion Systems; *Energy Fuels* **2006**, *20,* 1044-1056.
37. Merritt, P.M. *Diesel Exhaust Standard Phase 1: CRC Project NO. AVFL-10A, Final Report*; Prepared for Coordinating Research Council by Southwest Research Institute: San Antonio, TX, 2003.
38. Fanick, E.R. *Diesel Exhaust Standard Phase 2: CRC Project NO. AVFL-10B Final Report*; Prepared for Coordinating Research Council: Alpharetta, GA, 2005.
39. Grosjean, D.; Grosjean, E.; Gertler, A.W. On-Road Emissions of Carbonyls from Light-Duty and Heavy-Duty Vehicles; *Environ. Sci. Technol.* **2001**, *35,* 45-53.
40. Kirchstetter, T.W.; Singer, B.C.; Harley, R.A.; Kendall, G.R.; Chan, W. Impact of Oxygenated Gasoline Use on California Light-Duty Vehicle Emissions; *Environ. Sci. Technol.* **1996**, *30,* 661-670.
41. Schmitz, T.; Hassel, D.; Weber, F.-J. Determination of VOC-Components in the Exhaust of Gasoline and Diesel Passenger Cars; *Atmos. Environ.* **2000**, *34,* 4639-4647.
42. Siegl, W.O.; Hammerle, R.H.; Herrmann, H.M.; Wenclawiak, B.W.; Luers-Jongen, B. Organic Emissions Profile for a Light-Duty Diesel Vehicle; *Atmos. Environ.* **1999**, *33,* 797-805.
43. Sigsby, J.E.; Tejada, S.; Ray, W.; Lang, J.M.; Duncan, J.W. Volatile Organic Compound Emissions from 46 In-Use Passenger Cars; *Environ. Sci. Technol.* **1987**, *21,* 466-475.
44. Zhu, J.J.; Cao, X.-L.; Pigeon, R.; Mitchell, K. Comparison of Vehicle Exhaust Emissions from Modified Diesel Fuels; *J. Air & Waste Manage. Assoc.* **2003**, *53,* 67-76.
45. Vizuete, W.; Jeffries, H.; Biton, L.; Kioumourtzoglou, M.-A. *Regional Transport Modeling for East Texas, Project H60 Phase 2 Final Report*; Prepared by the University of North Carolina–Chapel Hill for the Texas Environmental Research Consortium: Houston, TX, 2006.
46. Lammel, G.; Cape, J.N. Nitrous Acid and Nitrite in the Atmosphere; *Chem. Soc. Rev.* **1996**, *25*, 361-369.
47. Kirchstetter, T.W.; Harley, R.A.; Littlejohn, D. Measurement of Nitrous Acid in Motor Vehicle Exhaust; *Environ. Sci. Technol.* **1996**, *30,* 2843-2849.
48. Kleffmann, J.; Kurtenbach, R.; Lorzer, J.; Wiesen, P.; Kalthoff, N.; Vogel, B.; Vogel, H. Measured and Simulated Vertical Profiles of Nitrous Acid—Part I: Field Measurements; *Atmos. Environ.* **2003**, *37,* 2949-2955.
49. Alicke, B.; Platt, U.; Stutz, J. Impact of Nitrous Acid Photolysis on the Total Hydroxyl Radical Budget during the Limitation of Oxidant Production/Pianura Padana Produzione di Ozono Study in Milan; *J. Geophys. Res.* **2002**, *107*, doi: 10.1029/2000JD000075.

50. Kleffmann, J.; Benter, T.; Wiesen, P. Heterogeneous Reaction of Nitric Acid with Nitric Oxide on Glass Surfaces Under Simulated Atmospheric Conditions; *J. Phys. Chem. A* **2004**, *108,* 5793-5799.
51. Zhou, X.; He, Y.; Huand, G.; Thornberry, T.; Carroll, M.A.; Bertman, S.B. Photochemical Production of Nitrous Acid on Glass Sample Manifold Surface; *Geophys. Res. Lett.* **2002**, *29*, doi: 10.1029/2002GL015080.
52. Gutzwiller, L.; Arens, F.; Baltensperger, U.; Gaeggeler, H.; Ammann, M. Significance of Semivolatile Diesel Exhaust Organics for Secondary HONO Formation; *Environ. Sci. Technol.* **2002**, *36,* 677-682.
53. Stemmler, K.; Ammann, M.; Donders, C.; Kleffmann, J.; George, C. Photosensitized Reduction of Nitrogen Dioxide on Humic Acid as a Source of Nitrous Acid; *Nature* **2006**, *440,* 195-198.
54. Lam, B.; Diamond, M.L.; Simpson, A.J.; Makar, P.A.; Truong, J.; Hernandez-Martinez, N.A. Chemical Composition of Surface Films on Glass Windows and Implications for Atmospheric Chemistry; *Atmos. Environ.* **2005**, *39,* 6578-6586.
55. Ammann, M.; Kalberer, M.; Jost, D.T.; Tobler, L.; Rossler, E.; Piguet, D.; Gäggeler, H.W.; Baltensperger, U. Heterogeneous Production of Nitrous Acid on Soot in Polluted Air Masses; *Nature* **1998**, *395,* 157-160.
56. Schurath, U.; Naumann, K.-H. Heterogeneous Processes Involving Atmospheric Particulate Matter; *Pure Appl. Chem.* **1998**, *70,* 1353-1361.
57. Bröske, R.; Kleffmann, J.; Wiesen, P. Heterogeneous Conversion of NO_2 on Secondary Organic Aerosol Surfaces: a Possible Source of Nitrous Acid (HONO) in the Atmosphere? *Atmos. Chem. Phys.* **2003**, *3*, 469-474.
58. Stemmler, K.; Ammann, M.; Elshorbany, Y.; Kleffmann, J.; Ndour, M.; D'Anna; B.; George, C.; Bohn, B. Light Induced Conversion of Nitrogen Dioxide into Nitrous Acid on Submicron Humic Acid Aerosol; *Atmos. Chem. Phys. Discuss.* **2007**, *7,* 4035-4064.
59. Reisinger, A.R. Observation of HNO_2 in the Polluted Winter Atmosphere: Possible Heterogeneous Production on Aerosols; *Atmos. Environ.* **2000**, *34,* 3865-3874.
60. Kleffman, J. Daytime Sources of Nitrous Acid (HONO) in the Atmospheric Boundary Layer; *Chem. Phys. Chem.* **2007**, *8,* 1137-1144.
61. Bejan, I.; El Aal, Y.A.; Barnes, I.; Benter, T.; Bohn, B.; Wiesen, P.; Kleffmann, J. The Photolysis of Ortho-Nitrophenols: a New Gas Phase Source of HONO; *Phys. Chem. Chem. Phys.* **2006**, *8,* 2028-2035.
62. Acker, K.; Febo, A.; Trick, S. Perrino, C.; Bruno, P.; Wiesen, P.; Möller, D.; Wieprecht, W.; Auel, R.; Giusto, M.; Geyer, A.; Platt, U.; Allegrini, I. Nitrous Acid in the Urban Area of Rome; *Atmos. Environ.* **2006**, *40,* 3123-3133.
63. Ziemba, L.D.; Dibb, J.E.; Griffin, R.J.; Anderson, C.H.; Whitlow, S.I.; Lefer, B.L.; Rappenglück, B.; Flynn, J. Heterogeneous Conversion of Nitric Acid to Nitrous Acid on the Surface of Primary Organic Aerosol in an Urban Atmosphere; *Atmos. Environ.*, in press.
64. Stutz, J.; Wong, K.-W.; Lawrence, L.; Flynn, J.H.; Rappenglück, B.; Lefer, B.; Ziemba, L.; Griffin, R. Nocturnal NO_3 Radical Chemistry in Houston, TX; *Atmos. Environ.*, in press.
65. Luke, W.T.; Kelley, P.; Lefer, B.L.; Flynn, J.; Rappenglück, B.; Leuchner, M.E.; Dibb, J.E.; Ziemba, L.D.; Anderson, C.H.; Buhr, M. Measurements of Primary Trace Gases and NO_y Composition during TRAMP; *Atmos. Environ.*, submitted for publication.
66. Mao, J.; Ren, X.; Chen, S.; Brune, W.H.; Chen, Z.; Martinez, M.; Harder, H.; Lefer, B.; Rappenglück, B.; Flynn, J.; Leuchner, M. Atmospheric Oxidation Capacity in the Summer of Houston 2006: Comparison with Summer Measurements in Other Metropolitan Studies; *Atmos. Environ.*, in press.
67. *TRAMP Data Analysis and Radical Chemistry Study, Project H86 Interim Report*; Prepared by the University of Houston for the Texas Environmental Research Consortium: Houston, TX, 2007.
68. Stockwell, W.R.; Kirchner, F.; Kuhn, M.; Seefeld, S. A New Mechanism for Regional Atmospheric Chemistry Modeling; *J. Geophys. Res.* **1997**, *102*, 25847-25879.
69. Sander, S.P.; Friedl, R.R.; Golden, D.M.; Kurylo, M.J.; Moortgat, G.K. Keller-Rudek, H.; Wine, P.H.; Ravishankara, A.R.; Kolb, C.E.; Molina, M.J.; Finlayson-Pitts, B.J.; Huie, R.E.; Orkin, V.L. *Chemical Kinetics and Photochemical Data for Use in Atmospheric Studies, Evaluation Number 15*, Jet Propulsion Laboratory (JPL) Publication 06-2; National Aeronautics and Space Administration; JPL California Institute of Technology: Pasadena, CA, 2006.
70. Madronich, S.; Flocke, S. In *Solar Ultraviolet Radiation—Modeling, Measurements & Effects*; Zerefos, C.S., Bais, A.F. Eds.; Springer-Verlag: Berlin, 1997; NATO ASI Series I: Global Environmental Change, Vol. 52, pp 23-48.
71. Chen S.; Ren X.; Mao J.; Chen Z.; Brune W.H.; Lefer B.; Rappenglück B.; Flynn J.; Olson J.; Crawford J.H. A Comparison of Chemical Mechanisms Based on TRAMP-2006 Field Data; *Atmos. Environ.*, in press.
72. Lei, W.; Zhang, R.; Tie, X.; Hess, P. Chemical Characterization of Ozone Formation in the Houston-Galveston Area: a Chemical-Transport Model Study; *J. Geophys. Res.* **2004**, *109*, doi: 10.1029/2003JD004219.
73. Sarwar, G.; Roselle, S.J.; Mathur, R.; Wyat, A.; Dennis, R.L.; Vogel, B. A Comparison of HONO Predictions with Observations from the Northeast Oxidant and Particle Study; *Atmos. Environ.* **2008**, *42,* 5760-5770.
74. Kanaya, Y.; Sadanaga, Y.; Matsumoto, J.; Sharma, U.K.; Hirokawa, J.; Kajii, Y.; Akimoto, H. Nighttime Observation of the HO_2 Radical by an LIF Instrument at Oki Island, Japan, and its Possible Origins; *Geophys. Res. Lett.* **1999**, *26,* 2179-2182.
75. Geyer, A.; Bächmann, K.; Hofzumahaus, A.; Holland, F.; Konrad, S.; Klüpfel, T.; Pätz, H.-W.; Perner, D.; Mihelcic, D.; Schäfer, H.-J.; Volz-Thomas, A.; Platt, U. Nighttime Formation of Peroxy and Hydroxyl Radicals during the BERLIOZ Campaign: Observations and Modeling Studies; *J. Geophys. Res.* **2003**, *108*, doi: 10.1029/2001JD000656.
76. Rubio, M.A.; Lissi, E.; Villena, G. Nitrite in Rain and Dew in Santiago City, Chile. Its Possible Impact on the Early Morning Start of the Photochemical Smog; *Atmos. Environ.* **2002**, *36,* 293-297.
77. Geyer, A.; Stutz, J. The Vertical Structure of OH-HO_2-RO_2 Chemistry in the Nocturnal Boundary Layer: a One-Dimensional Model Study; *J. Geophys. Res.* **2004**, *109*, doi: 10.1029/2001JD004425.
78. Dentener, F.; Williams, J.; Metzger, S. Aqueous Phase Reaction of HNO_4: the Impact on Tropospheric Chemistry; *J. Atmos. Chem.* **2002**, *41,* 109-134.
79. Williams, J.E.; Dentener, F.J.; Van den Berg, A.R. The Influence of Cloud Chemistry on HO_x and NO_x in the Marine Boundary Layer: a 1-d Modeling Study; *Atmos. Chem. Phys. Discuss.* **2001**, *1,* 277-335.
80. Kim, S.; Huey, L.G.; Stickel, R.E.; Tanner, D.J.; Crawford, J.H.; Olson, J.R.; Chen, G.; Brune, W.H.; Ren, X.; Lesher, R.; Wooldridge, P.J.; Bertram, T.; Perring, A.; Cohen, R.C.; Lefer, B.L.; Shetter, R.E.; Avery, M.; Diskin, G.; Sokolik, I. Measurement of HO_2NO_2 in the Free Troposphere during the Intercontinental Chemical Transport Experiment–North America 2004; *J. Geophys. Res.* **2007**, *112*, doi: 10.1029/2006JD007676.

About the Authors

Dr. Eduardo Olaguer is a senior research scientist at the Houston Advanced Research Center. Dr. Bernhard Rappenglück is an associate professor and Dr. Barry Lefer is an assistant professor of Atmospheric Chemistry at the University of Houston. Dr. Jochen Stutz is an associate professor of Atmospheric and Oceanic Sciences at the University of California–Los Angeles. Dr. Jack Dibb is a research associate professor of Tropospheric Chemistry at the University of New Hampshire. Dr. Robert Griffin is an associate professor of Civil and Environmental Engineering at Rice University. Dr. William H. Brune is a professor of Meteorology at Pennsylvania State University. Dr. Maxwell Shauck is Director of the Institute for Air Science at Baylor University. Dr. Martin Buhr is President and Principal Scientist at Air Quality Design, Inc. Dr. Harvey Jeffries is a professor and Dr. William Vizuete is an assistant professor of Atmospheric and Aquatic Sciences at the University of North Carolina–Chapel Hill. Dr. Joseph P. Pinto is an atmospheric scientist at the EPA National Center for Environmental Assessment. Please address correspondence to: Dr. Eduardo Olaguer, Houston Advanced Research Center, 4800 Research Forest Drive, The Woodlands, TX 77381; phone: +1-281-364-4020; fax: +1-281-363-7935; e-mail: eolaguer@harc.edu.